Scientific Research Publishing

Journal of High Energy Physics, Gravitation and Cosmology, 2022, 8, 724-767
https://www.scirp.org/journal/jhepgc
ISSN Online: 2380-4335
ISSN Print: 2380-4327

New Solutions of Tolman-Oppenheimer-Volkov-Equation and of Kerr Spacetime with Matter and the Corresponding Star Models

Jan Helm

Technical University of Berlin, Berlin, Germany
Email: jan.helm@alumni.tu-berlin.de

How to cite this paper: Helm, J. (2022) New Solutions of Tolman-Oppenheimer-Volkov-Equation and of Kerr Spacetime with Matter and the Corresponding Star Models. *Journal of High Energy Physics, Gravitation and Cosmology*, **8**, 724-767.
https://doi.org/10.4236/jhepgc.2022.83052

Received: March 7, 2022
Accepted: July 25, 2022
Published: July 28, 2022

Abstract

The Tolman-Oppenheimer-Volkov (TOV) equation is solved with a new ansatz: the external boundary condition with mass M_0 and radius R_1 is dual to the internal boundary condition with density ρ_{bc} and inner radius r_i, and the two boundary conditions yield the same result. The inner boundary condition is imposed with a density ρ_{bc} and an inner radius r_i, which is zero for the compact neutron stars, but non-zero for the shell-stars: stellar shell-star and galactic (supermassive) shell-star. Parametric solutions are calculated for neutron stars, stellar shell-stars, and galactic shell-stars. From the results, an M-R-relation and mass limits for these star models can be extracted. A new method is found for solving the Einstein equations for Kerr space-time with matter (extended Kerr space-time), *i.e.* rotating matter distribution in its own gravitational field. Then numerical solutions are calculated for several astrophysical models: white dwarf, neutron star, stellar shell-star, and galactic shell-star. The results are that shell-star star models closely resemble the behaviour of abstract black holes, including the Bekenstein-Hawking entropy, but have finite redshifts and escape velocity $v < c$ and no singularity.

Keywords

General Relativity, Tolman-Oppenheimer-Volkov Equation, Neutron Stars, Shell Stars

1. Introduction

In General Relativity, one of the most important applications is to calculate the mass distribution and the space-time metric for a given equation-of-state of a stellar model.

Without rotation, one has spherical symmetry and then the Tolman-Oppen-Heimer-Volkov (TOV) equation in radius r, which is derived directly from the Einstein equations (see [1]), is being used. The TOV equation consists originally of 2 coupled non-linear ordinary differential equations (odeq) of degree 1 in r for mass $M(r)$ and density $\rho(r)$, where $4\pi r^2\rho(r) = M(r)$, and can be transformed into one ordinary differential equation of degree 2 for $M(r)$ by eliminating $\rho(r)$.

The boundary condition is imposed normally at $r = 0$ with $M(0) = 0$ and $\rho(0) = \rho_0$, where ρ_0 is the maximal density. Then the TOV-equation for $M(r)$ is solved with this boundary condition at $r = 0$ for $M(r)$ and $M'(r)$, which gives the total mass $M_0(\rho_0)$ and the total radius $R(\rho_0)$, and a mass-radius relation $M_0(R)$.

The predominant view of the neutron stars and stellar black-holes is, that neutron stars obey an equation-of state (eos) of an interacting-fluid model [2], which solutions of the TOV equation up to about $M = 3M_{sun}$. For larger masses, it is assumed that only a black-hole solution remains. This is based on the so-called Oppenheimer limit for the radius of a compact mass

$R_{\lim} = \frac{9}{8}r_s = \frac{9MG}{4c^2}$: for a smaller compact object, the density at the center becomes infinite.

The new ansatz presented here is the extended (inner) boundary condition at $r = r_i$ with the non-zero inner radius r_i, $M(r_i) = 0$ and $\rho(r_i) = \rho_0$, *i.e.* the star becomes a shell-star with an (almost) void interior. With the parameters r_i and ρ_0, this ansatz generates a 2-parametric solution manifold, where, because of energy minimization, the stable physical solution is the one with minimal r_i for a given ρ_0, which determines the total mass $M_0(r_i, \rho_0)$ and the total radius $R(r_i, \rho_0)$. This ansatz circumvents the Oppenheimer limit, because the mass is non-compact, and the density at the center is zero. It yields valid solutions of the TOV-equation with a continuous mass-radius relation $M_0(R, r_i)$.

The Oppenheimer limit $R_{\lim} = \frac{9}{8}r_s = \frac{9MG}{4c^2}$ is deduced from the maximum pressure at $r = 0$:

$$P(0) = \rho_0 c^2 \frac{1-\sqrt{1-\frac{r_s}{R}}}{3\sqrt{1-\frac{r_s}{R}}-1}$$

The dual (outer) boundary condition is the one at $r = R$ with $M = M_0$ and $\rho = \rho_{bc}$, where ρ_{bc} depends on the equation-of-state (eos): for neutron stars with interacting nucleon fluid with the equilibrium nucleon density ρ_c, and for nucleon Fermi-gas (stellar shell-stars) $\rho_{bc} = 0$.

The 2 parameters R and M_0 in the dual outer boundary condition correspond uniquely to the 2 parameters r_i and ρ_0 in the inner boundary condition.

With rotation, one has an axisymmetric model in the variables r and θ (azimuthal angle), and has to solve the Einstein equations in these 2 coordinates. In

vacuum, the corresponding solution is the Kerr space-time in r and θ.

With mass, a good starting point is using the extended Kerr space-time in Boyer-Lindquist coordinates with correction-factor functions $A0$, …, $A4$ and $B0$, …, $B4$ and the mass $M(r, \theta)$ as variables and insert this into the Einstein equations.

Setting $Bi = 0$, 4 of the 10 Einstein equations become trivial and one is left with 6 partial-differential equations (pdeq) in r and θ for the 6 variables $A0$, …, $A4$ and M.

The (outer) boundary condition here at the effective star radius R with total mass M_0 is: $Ai = 1$, $M = M_0$ and $\partial_r Ai = 0$, $\partial_r M = 0$, as the density becomes 0 and the space-time becomes the normal Kerr space-time in vacuum.

Now, with rotation, we have a new model parameter, the angular velocity ω, to which corresponds a third parameter in the outer boundary condition: (outer) ellipticity ΔR_1, where $R_{1x} = R_{1y} - \Delta R_1$ and R_{1x} and R_{1y} are the equatorial and the polar radius. As in the TOV-case, here to the 3 parameters R_{1y}, M_0 and ΔR_1 correspond the 3 inner parameters r_{iy}, ρ_0 and Δr_i.

So here we get a 3-parametric solution manifold, and as in the spherical case, for a given total mass M_0 we have to find the stable physical solution. As before, these will be the ones with minimal riy and among them the one with minimal mean energy density: this defines the inner ellipticity Δr_i. In all considered cases, it can be shown numerically, that such a (non-trivial) minimum exists.

The paper is organized as follows.

In 2 we present the mathematical setup, in 3 the equations for the extended Kerr space-time with rotation, in 4 the solution algorithm for it. In 5 the TOV-equation is introduced, in 6 the equation-of-state for the nucleon fluid and nucleon gas. In 7 the results for the TOV-equation are shown: the parametric solution manifold in 7.1. and the case study for typical stars in 7.2. In 8 the results for the extended Kerr space-time with rotation are presented for three typical star configurations: compact neutron star, stellar shell-star, and galactic shell-star.

2. The Kerr Space-Time, Schwarzschild Space-Time, Einstein Equations

Using the Minkowski metric $\eta_{\mu\nu}$ $\eta_{\mu\nu} = \mathrm{diag}(1,-1,-1,-1)$, the Kerr space-time metric in original Kerr coordinates (u, θ, ϕ) has the line element [1] [3]

$$\begin{aligned} \mathrm{d}s^2 = &\left(1-\frac{rr_s}{r^2+a^2\cos^2\theta}\right)\left(\mathrm{d}u + a\sin^2\theta\,\mathrm{d}\varphi\right)^2 \\ &-2\left(\mathrm{d}u + a\sin^2\theta\,\mathrm{d}\varphi\right)\left(\mathrm{d}r + a\sin^2\theta\,\mathrm{d}\varphi\right) \\ &-\left(r^2+a^2\cos^2\theta\right)\left(\mathrm{d}\theta^2 + \sin^2\theta\,\mathrm{d}\varphi\right) \end{aligned} \tag{1}$$

where $r_s = \frac{2GM}{c^2}$ is the Schwarzschild radius, and $a = \frac{J}{Mc}$ is the angular momentum radius (amr), a has the dimension of a distance: $[a] = [r]$, and J is the angular momentum.

With this line element the Kerr metric tensor $g_{\mu\nu}$ is as follows: [3]

$$g_{\mu\nu}=\begin{pmatrix} 1-\dfrac{rr_s}{\rho_{12}} & -1 & 0 & -\dfrac{rr_s a\sin^2\theta}{\rho_{12}} \\ & 0 & 0 & -a\sin^2\theta \\ & & -\rho_{12} & 0 \\ & & & g_{33} \end{pmatrix} \tag{2}$$

with the abbreviations $\rho_{12}=r^2+a^2\cos^2\theta$ and $g_{33}=-\sin^2\theta\left(r^2+a^2+\dfrac{rr_s a^2\sin^2\theta}{\rho_{12}}\right)$.

In the limit $a\to 0$ the Schwarzschild space-time in advanced Eddington-Finkelstein coordinates emerges:

$$\mathrm{d}s^2=\left(1-\frac{r_s}{r}\right)\mathrm{d}u^2-2\mathrm{d}u\,\mathrm{d}r-r^2\left(\mathrm{d}\theta^2+\sin^2\theta\,\mathrm{d}\varphi\right) \tag{3}$$

This form of the Schwarzschild line element has the advantage in comparison with the original line element

$$\mathrm{d}s^2=\left(1-\frac{r_s}{r}\right)c^2\mathrm{d}t^2-\frac{\mathrm{d}r^2}{1-\dfrac{r_s}{r}}-r^2\left(\mathrm{d}\theta^2+\sin^2\theta\,\mathrm{d}\varphi\right) \tag{3a}$$

that the (apparent) singularity at $r=r_s$ is missing.

The same is valid for the original Kerr space-time: the denominator ρ_{12} has no zeros, there is no singularity in g_{ab}, which makes it more well-behaved numerically.

Alternatively, in Boyer-Lindquist-coordinates: [3]

$$g_{\mu\nu}=\begin{pmatrix} 1-\dfrac{rr_s}{\rho_{12}} & 0 & 0 & \dfrac{rr_s a\sin^2\theta}{\rho_{12}} \\ & -\rho_{12}/\Lambda_{12} & 0 & 0 \\ & & -\rho_{12} & 0 \\ & & & -\sin^2\theta\left(r^2+a^2+\dfrac{rr_s a^2\sin^2\theta}{\rho_{12}}\right) \end{pmatrix} \tag{4}$$

with the line element

$$\begin{aligned}\mathrm{d}s^2=&\left(1-\frac{rr_s}{r^2+a^2\cos^2\theta}\right)(\mathrm{d}t)^2+\left(\frac{2rr_s a\sin^2\theta}{r^2+a^2\cos^2\theta}\right)\mathrm{d}t\,\mathrm{d}\varphi\\ &-\left(\frac{r^2+a^2\cos^2\theta}{r^2-rr_s+a^2}\right)\mathrm{d}r^2-\left(r^2+a^2+\frac{rr_s a^2\sin^2\theta}{r^2+a^2\cos^2\theta}\right)\sin^2\theta\,\mathrm{d}\varphi^2\\ &-\left(r^2+a^2\cos^2\theta\right)\left(\mathrm{d}\theta^2\right)\end{aligned} \tag{4a}$$

with the abbreviation $\Lambda_{12}=r^2-rr_s+a^2$. Here, Λ_{12} has zeros at the inner/outer horizon $r=(r_s/2)\pm\sqrt{(r_s/2)^2-a^2\cos^2\theta}$, so for numerical calculations the singularity has to be removed by adding a small ε: $\Lambda_{12}=\sqrt{\left(r^2-rr_s+a^2\right)^2+\varepsilon^2}$.

In the limit $a \to 0$ the Schwarzschild space-time in the standard form (4) emerges.

The Einstein field equations with the above Minkowski metric are:

$$R_{\mu\nu} - \frac{1}{2} g_{\mu\nu} R_0 - \Lambda g_{\mu\nu} = -\kappa T_{\mu\nu} \tag{5}$$

where $R_{\mu\nu}$ is the Ricci tensor, R_0 the Ricci curvature, $\kappa = \frac{8\pi G}{c^4}$, $T_{\mu\nu}$ is the energy-momentum tensor, Λ is the cosmological constant (in the following neglected, *i.e.* set 0),

with the Christoffel symbols (second kind)

$$\Gamma^{\lambda}_{\mu\nu} = \frac{1}{2} g^{\lambda\kappa} \left(\frac{\partial g_{\kappa\mu}}{\partial x^{\nu}} + \frac{\partial g_{\kappa\nu}}{\partial x^{\mu}} - \frac{\partial g_{\mu\nu}}{\partial x^{\kappa}} \right) \tag{6}$$

and the Ricci tensor

$$R_{\mu\nu} = \frac{\partial \Gamma^{\rho}_{\mu\rho}}{\partial x^{\nu}} - \frac{\partial \Gamma^{\rho}_{\mu\nu}}{\partial x^{\rho}} + \Gamma^{\sigma}_{\mu\rho} \Gamma^{\rho}_{\sigma\nu} - \Gamma^{\sigma}_{\mu\nu} \Gamma^{\rho}_{\sigma\rho} \tag{7}$$

The crucial part of the extended Kerr solution is the expression for the energy-momentum tensor $T_{\mu\nu}$. As usual, one uses the formula for the perfect fluid [1, (45.3)]:

$$T_{\mu\nu} = \left(\rho + \frac{P}{c^2} \right) u_{\mu} u_{\nu} - P g_{\mu\nu} \tag{8}$$

where P and ρ is the pressure and density, u_{μ} is the covariant velocity 4-vector.

In the Schwarzschild case, when deriving the TOV-equation, one sets the spatial contravariant velocity components to 0: $u^i = 0$, in the Kerr case the tangential velocity $u^3 = u^{\varphi} \neq 0$.

For the velocity one has:

$u^3 = r\omega = r\frac{aMc}{I}$, where I is the moment of inertia and ω the angular velocity, $I = f_I M R_1^2$, so

$$u^3 = \frac{1}{f_I} \frac{acr}{R_1^2}$$

for a homogeneous sphere $I = \frac{2}{5} MR^2$ *i.e.* $f_I = \frac{2}{5}$, for a thin shell $I = \frac{2}{3} MR^2$ *i.e.* $f_I = \frac{2}{3}$, for a disc $I = \frac{1}{2} MR^2$.

If we make the obvious assumption that the star rotates as a whole, *i.e.* with constant angular velocity, then the moment of inertia I becomes r-dependent, like the mass M:

$$M(r) = \int_0^r \rho(r_1) 3 r_1^2 \mathrm{d}r_1 \tag{9}$$

$$I(r) = \int_0^r \rho(r_1) 3 r_1^4 \mathrm{d}r_1$$

The factor 3 in the integral instead of the usual 4π comes from the dimensionless calculation in "sun units" (see below).

The amr a also becomes r-dependent:

$$a(r)=\frac{J}{Mc}=\frac{I(r)\omega}{M(r)c}$$

In the relativistic axisymmetric case with rotation with angular velocity ω, u^{μ} has the form [4]: $u^{\mu}=u^{0}(1,0,0,w)$

$$u^{\mu}=\left(u^{0},0,0,\omega u^{0}\right)$$

Now u^{0} is calculated from the condition

$$c^{2}=g_{\mu\nu}u^{\mu}u^{\nu}$$

and the covariant velocity from

$$u_{\mu}=g_{\mu\nu}u^{\nu}$$

The resulting expression for u^{0} is (A_i are the Kerr correction-factors, mass $M_1[r_1]$, moment of inertia $I_1[r_1]$): (9a)

$$\begin{aligned}u^{0}=&\left(A_{0}(r_{1},\theta)\sqrt{\left(\frac{r_{1}M_{1}(r_{1})^{3}}{\omega^{2}I_{1}(r_{1})^{2}\cos^{2}(\theta)+r_{1}^{2}M_{1}(r_{1})^{2}}-1\right)^{2}}\right.\\&-\frac{r_{1}\omega^{4}I_{1}(r_{1})^{2}M_{1}(r_{1})\cos^{4}(\theta)A_{3}(r_{1},\theta)}{\omega^{2}I_{1}(r_{1})^{2}\cos^{2}(\theta)+r_{1}^{2}M_{1}(r_{1})^{2}}\\&-\frac{\omega^{4}I_{1}(r_{1})^{2}\sin^{2}(\theta)A_{3}(r_{1},\theta)}{M_{1}(r_{1})^{2}}-r_{1}^{2}\omega^{2}\sin^{2}(\theta)A_{3}(r_{1},\theta)\\&\left.+\frac{2\omega^{2}\sqrt{I_{1}(r_{1})^{2}}M_{1}(r_{1})\sqrt{M_{1}(r_{1})^{2}}\sin^{2}(\theta)A_{4}(r_{1},\theta)}{\omega^{2}I_{1}(r_{1})^{2}\cos^{2}(\theta)+r_{1}^{2}M_{1}(r_{1})^{2}}\right)^{-1}\end{aligned}$$

The state equation for the pressure P for the nucleon gas has the form

$$P=c_{1}\rho^{\gamma}$$

or in the dimensionless form with a critical density ρ_c and dimensionless pressure P_1 and density ρ_1

$$P_{1}:=\frac{P}{c^{2}\rho_{c}}=k_{1}\left(\frac{\rho}{\rho_{c}}\right)^{\gamma}=k_{1}(\rho_{1})^{\gamma}\tag{10}$$

For the horizon, with rotation there is the inner and the outer horizon ($M = M_0$)

$$r_{-}=\frac{M_{0}}{2}-\sqrt{\left(\frac{M_{0}}{2}\right)^{2}-a^{2}}$$

$$r_{+}=\frac{M_{0}}{2}+\sqrt{\left(\frac{M_{0}}{2}\right)^{2}-a^{2}}$$

3. The Equations for the Extended Kerr Space-Time

The solution process starts with the metric tensor $g_{\mu\nu}$ in original Edding-

ton-Finkelstein-coordinates, with 6 non-zero components, corresponding correction-factor functions $A0$, …, $A5$, and additive correction functions $B0$, …, $B3$ for the zero components.

$$g_{\mu\nu}=\begin{pmatrix}\left(1-\frac{rr_s}{\rho_{12}}\right)A0 & -A3 & B1 & -\frac{rr_s a\sin^2\theta}{\rho_{12}}A4\\ & B0 & B2 & -a\sin^2\theta A5\\ & & -\rho_{12}A1 & B3\\ & & & -A2\sin^2\theta\left(r^2+a^2+\frac{rr_s a^2\sin^2\theta}{\rho_{12}}\right)\end{pmatrix} \tag{11}$$

and alternatively in Boyer-Lindquist-coordinates, corresponding correction-factor functions $A0$, …, $A4$, and additive correction functions $B0$, …, $B4$ for the zero components

$$g_{\mu\nu}=\begin{pmatrix}\left(1-\frac{rr_s}{\rho_{12}}\right)A0 & B0 & B1 & \frac{rr_s a\sin^2\theta}{\rho_{12}}A4\\ & -A1\rho_{12}/\Lambda_{12} & B2 & B3\\ & & -\rho_{12}A2 & B4\\ & & & -A3\sin^2\theta\left(r^2+a^2+\frac{rr_s a^2\sin^2\theta}{\rho_{12}}\right)\end{pmatrix} \tag{12}$$

The equations are the 10 Einstein equations eqR00, eqR11, eqR22, eqR33, eqR12, eqR23, eqR31, eqR01, eqR02, eqR03 in the (dimensionless) variables relative radius $r_1=\frac{r}{r_{ss}}$ and complementary azimuth angle $\theta_1=\frac{\pi}{2}-\theta$ with energy tensor $T_{\mu\nu}$ from (8) and the state equation $P_1=k_1(\rho_1)^\gamma$ for the relative pressure P_1 and the relative density ρ_1. We are using the so called "sun units" $r_{ss}=r_s(sun)$, $M_s=M(sun)$, $\rho_s=\frac{M_s}{4\pi r_{ss}^3}$, $P_s=\rho_s c^2$ for radius r, mass M, density ρ, and pressure P, respectively.

In "sun units" the original angle differential $\mathrm{d}\Omega=4\pi\sin\theta r^2\mathrm{d}r\mathrm{d}\theta$ is transformed into $\mathrm{d}\Omega=3\cos\theta r^2\mathrm{d}r\mathrm{d}\theta$, as for $\theta=0,\cdots,\pi/2$, $r=0,\cdots,1$: $\int\mathrm{d}\Omega=1$.

Also, all equations and variables are symmetric (even) in θ: $Ai(-\theta)=Ai(\theta)$.

From now on we skip the index of the dimensionless variables and use the original notation, e.g. r instead of r_1.

Furthermore, we adopt the Boyer-Lindquist coordinates and the metric tensor (12).

In sun units, the Boyer-Lindquist metric tensor becomes:

$$g_{\mu\nu}=\begin{pmatrix}\left(1-\frac{rM_0}{\rho_{12}}\right)A0 & B0 & B1 & \frac{rM_0 a\cos^2\theta}{\rho_{12}}A4\\ & -A1\rho_{12}/\Lambda_{12} & B2 & B3\\ & & -\rho_{12}A2 & B4\\ & & & -A3\cos^2\theta\left(r^2+a^2+\frac{rM_0 a^2\cos^2\theta}{\rho_{12}}\right)\end{pmatrix} \tag{12a}$$

$$\rho_{12} = r^2 + a^2 \sin^2\theta$$

$$\Lambda_{12} = r^2 - rM_0 + a^2$$

where M_0 is the mass in sun units.

The 10 Einstein equations have a distinctive structure: there are 6 primary variables $A0$, $A2$, $A3$, $A4$, $B1$, $B4$ with highest derivative ∂_{rr} and 4 secondary variables $A1$, $B2$, $B0$, $B3$ with highest derivative ∂_r. Primary variables have boundary conditions for the variable and its r-derivative, secondary variables only for the variable itself.

This structure is dual in θ: again there are 6 θ-primary and 4 θ-secondary variables.

6 of Einstein equations contain only one 2-derivative ∂_{rr} of a primary variable: eqR03($\partial_{rr}A4$), eqR22($\partial_{rr}A2$), eqR00($\partial_{rr}A0$), eqR33($\partial_{rr}A3$), eqR02($\partial_{rr}B1$), eqR23 ($\partial_{rr}B4$) 3 contain only 2-derivatives of a secondary variable: eqR12, eqR01, eqR31, eqR11 contains all derivatives ∂_{rr} of a primary variable.

If we make the ansatz $Bi = 0$, several of the eqRij become identically 0, and we get the 6 equations eqR00, eqR11, eqR22, eqR33, eqR03, eqR12 for the 6 variables Ai and ρ, with the highest derivatives resp. $\partial_{rr}A0$, $\partial_{\theta\theta}A1$, $\partial_{rr}A2$, $\partial_{rr}A3$, $\partial_{rr}A4$, ($\partial_{rr}A2$, $\partial_{\theta\theta}A1$).

Thus, we are left with the 6 differential equations degree 2 in r, θ non-linear (quartic) in variables Ai and their 1-derivatives and linear in ρ, ρ^γ.

In total, we have 6 algebro-differential eqs for 6 variables Ai and ρ (ρ enters only algebraically).

We can add 2 dependent equations eqR41 == $D_\mu T^{\mu 1} = 0$ and eqR42 == $D_\mu T^{\mu 2} = 0$, from the covariant continuity equations $D_\mu T^{\mu\nu} = 0$, where $D_\lambda T^{\mu\nu} = \partial_\lambda T^{\mu\nu} + \Gamma^\mu_{\lambda\kappa} T^{\kappa\nu} + \Gamma^\nu_{\lambda\kappa} T^{\mu\kappa}$ is the gravitational covariant derivative.

In eqR41 ρ enters with $\partial_r\rho$, in eqR42 ρ enters with $\partial_\theta\rho$.

So, alternatively, we have the diff. equations eqR00, eqR11, eqR22, eqR33, eqR03, eqR41, with the highest derivatives resp. $\partial_{rr}A0$, $\partial_{\theta\theta}A1$, $\partial_{rr}A2$, $\partial_{rr}A3$, $\partial_{rr}A4$, $\partial_r\rho$ (diff. eq. degree 1 in r for ρ) or the diff. equations eqR00, eqR11, eqR22, eqR33, eqR03, eqR42, with the highest derivatives resp. $\partial_{rr}A0$, $\partial_{\theta\theta}A1$, $\partial_{rr}A2$, $\partial_{rr}A3$, $\partial_{rr}A4$, $\partial_\theta\rho$ (diff. eq. degree 1 in θ for ρ).

In the Schwarzschild spacetime $\omega = 0$ and $a = 0$, we have spherical symmetry, no dependence on θ, and the TOV-equation can be derived from the non-trivial eqR00, eqR11, eqR22, eqR41.

We impose an r-θ-analytic boundary condition for Ai, $\partial_r Ai$, at $r = R_1$(R_1 is the star radius):

$Ai = 1$, $\partial_r A0 = 0$, $\partial_r A2 = 0$, $\partial_r A3 = 0$, $\partial_r A4 = 0$. For $A1$, there is no differential boundary condition, as $\partial_r A1$ is the highest r-derivative, for ρ there is no boundary condition at all, because r is algebraic in the equations, but there is an integral condition:

$$M(R_1) = \int_0^{\pi/2}\int_0^{R_1} \rho(r_1,\theta) 3r_1^2 \cos\theta \, \mathrm{d}r_1 \, \mathrm{d}\theta = M_0 : \text{integral}(\rho) = \text{total mass} = M_0.$$

In order to avoid the clumsy integral condition for ρ, we can introduce the mass M as a variable:

$$M(r,\theta)=\int_0^r \rho(r_1,\theta)3r_1^2\mathrm{d}r_1$$

$M(r)=\int_0^{\pi/2} M(r,\theta)\mathrm{d}\theta=\int_0^{\pi/2}\int_0^r \rho(r_1,\theta)3r_1^2\,\mathrm{d}r_1\cos\theta\mathrm{d}\theta$ is the mass of the sphere(r) and

$$\partial_r M(r,\theta)=\rho(r,\theta)3r^2$$

For $M(r, \theta)$ we impose the boundary condition at $r = R_1$:

$M(R_1,\theta)=M_0$, $\partial_r M(R_1,\theta)=0$ (*i.e.* density ρ is zero at boundary, and total mass M_0).

So, if we take the diff. equations eqR00, eqR11, eqR22, eqR33, eqR03, eqR41 and replace $\rho(r,\theta)$ by $\partial_r M(r,\theta)$, we have 6 diff.equations in r, θ of degree 2, for the variables $Ai(r, \theta)$ (metric correction factors = mcf) and the mass $M(r, \theta)$, with the highest derivative $\partial_{rr}M(r, \theta)$ in M.

According to the Cauchy-Kovalevskaya theorem there exists then a unique solution in a region $R_1 > r > r_i$ within the boundary. Inside the region $r_i > r > 0$ we can enforce the vacuum Kerr-spacetime with the trivial solution $Ai = 1$, $\rho = 0$, *i.e.* there is no matter there, r_i the inner radius.

The Cauchy-Kovalevskaya theorem guarantees the existence of a mathematical solution outside the horizon, but for a physical solution we must have $r \geq 0$ (meaning $\partial_r M(r,\theta)>0$) and $M(r,\theta)\leq 0$ for $r \leq r_i$: the mass must become non-positive at the inner radius.

Therefore, for certain $\{M_0, R_1\}$ values there will be no physical solution, even for the TOV equation.

4. The Solving Process for the Extended Kerr Space-Time

In addition to the fundamental dual parameters $\{r_i, \rho_i\}$ corresponding to $\{R_1, M_0\}$ in the rotation-free TOV-case, in the Kerr-case there is the new fundamental parameter Δr_i (inner ellipticity for inner boundary condition), resp. ΔR_1 (outer ellipticity for outer boundary condition), and the angular velocity ω. The outer radii are

$R_{x1} = R_1 - \Delta R_1$ and $R_{y1} = R_1$, the latter equality arising from the fact that centrifugal distortion acts only in the x-direction (the y-axis being the rotation axis). The inner radii are correspondingly $r_{xi} = r_i - \Delta r_i$, $r_{yi} = r_i$.

The r-θ-slicing algorithm with an Euler-step obeys the iterative procedure with slice step size h_1 in r, and step size h_2 in θ, starting with the r-boundary at $r = R_1$ (slice $n = 0$).

The transition from slice n to $n + 1$ proceeds as follows.

At slice n all variables and 1-derivatives are known from the previous step, 2-derivatives $\partial_{rr}Ai$, and ρ are calculated from the 6 equations.

At slice $n + 1$ the variables and 1-derivatives are calculated by Euler-formula (or Runge-Kutta)

$$Ai_{n+1} = Ai_n + h_1\partial_r Ai_n$$

$$\partial_r Ai_{n+1} = \partial_r Ai_n + h_1 \partial_{rr} Ai_n$$

The 2-derivatives $\partial_{rr}Ai$, $\partial_{rr}Bi$ and ρ are again calculated from the 6 significant equations with variables and 1-derivatives inserted from above.

The θ-slicingr-backward algorithm with an Euler-step obeys the iterative procedure with slice step size h_1 in θ as above for r, starting with $\theta = 0$, and solves an ordinary differential equation in r in each θ -step. The boundary condition for the r-odeq is set at $r = R_1(\theta)$ (the outer ellipse radius) with $Ai = 1$, $M = M_0 My0(\theta)$, $\partial_r Ai = 0$, $\partial_r M = 3(R_1)^2 \rho_{bc}$, where ρ_{bc} is the outer boundary value for the density, $\rho_{bc} = 0$ for the (non-interacting) neutron-gas in a shell-star and $\rho_{bc} > 0$, $\rho_{bc} = \rho_{equilibrium}$ for the (interacting) neutron fluid in a neutron star. $My0(\theta)$ is the mass-form-factor with the condition $\int_0^{\pi/2} My0(\theta)\mathrm{Cos}(\theta)\mathrm{d}\theta = 1$, *i.e.* the overall mass at the outer boundary is M_0. The inner radius $r_i(\theta)$ is reached, when $My0(\theta) = 0$.

The alternative (dual) θ-slicingr-forward algorithm starts with the boundary condition at

$$r = r_i(\theta)$$

$Ai = 1$, $M = 0$, $\partial_r Ai = 0$, $\partial_r M = 3(r_i)^2 \rho_{bc}$, where $\rho_{bc} = \rho_i$ is the inner boundary value for the density, ρ_i is approximately the inner (maximum) density $\rho(r_i)$ from the corresponding TOV-equation, the value must be adapted, so that the resulting total mass is M_0. For the compact neutron star the inner radius $r_i(\theta)$ is zero.

In the θ-slicingr-backward algorithm one starts with the outer boundary being the ellipsoid $r = R(\theta, \Delta R_1)$, where ΔR_1 is the outer ellipticity of the star. In the θ-slicingr-forward algorithm one starts with the inner boundary being the ellipsoid $r = r_i(\theta, \Delta r_i)$, where Δr_i is the inner ellipticity of the star.

At the inner boundary the tangential pressure is uniform, so the density is also uniform and equal to the maximum density, $\rho(\theta) = \rho_i$.

In the actual calculation we were using the θ-slicingr-backward algorithm, because here the boundary condition $M = M_0$ is achieved automatically, when one starts with $My_0(\theta) = M_0$.

The odeqs in *r*consist of the 6 significant Einstein equations *eqR00*, *eqR11*, *eqR22*, *eqR33*, *eqR03*, *eqR41* for the six variables $A0(r, \theta)$, $A1(r, \theta)$, $A2(r, \theta)$, $A3(r, \theta)$, $A4(r, \theta)$, $M(r, \theta)$ with $\theta = \theta_i$ and θ-derivatives calculated by Euler-step from the preceding q-slice. For $i = 0$ *i.e.* $\theta = 0$ the θ-derivatives are taken from start values for all variables, which normally represent the corresponding TOV-solution (here only $A0(r)$, $A1(r)$, $M(r)$ are non-trivial and do not depend on θ). The odeqs are highly non-linear algebraic differential equations and hard to solve numerically with classical methods for linear odeqs extended by an algebraic equation solver. In the case of a nonlinear odeq-system one uses an Euler or Runge-Kutta method and calculates in each step the highest derivatives with a numerical algebraic equation solver. As an alternative one can use minimization of the least-squares-error in the highest derivatives instead of a numerical algebraic equation solver. Minimization has also the advantage that one can minim-

ize the complete set of Einstein equations plus the 2 additional continuity equations *eqR41*, *eqR42* in the error goal function instead of the 6 significant equations, which improves the stability of the solution (e.g. in case of degeneracy).

The numerical error of the algorithm is calculated from $\sum_i \left\{ (eq_i)^2, i = 1, \cdots, n \right\}$ *i.e.* the Euclidean norm of the equation values (the right side of the Einstein equations being 0). The error is calculated over the lattice $\{r_i, \theta_j\}$ as median, mean or maximum. In the internal loop of the algorithm over r_i at fixed θ_j, the solution of the algebraic discretised Einstein-equation is achieved by square-root error minimization, so it is essential to avoid singularities, e.g. at the horizon and the pseudo-singularity at $\theta = 0$. This is achieved by selecting appropriate analytic *convergence factors* for the (left side of) the Einstein equations. As the equations are to be zeroed for the solution, the convergence factors do not change the solution of course, but they cancel the numerical singularities, which could otherwise jeopardize the numerical convergence of the algorithm.

The actual calculation was carried out in Mathematica using its symbolic and numerical procedures. In the first stage, the Einstein equations were derived from the ansatz for $g_{\mu\nu}$ from section 2 and simplified automatically. The arising complexity of the equations is such, that it is practically impossible to handle them manually: the Mathematica function *LeafCount*, which returns the number of terms in the equation, gives the complexity of *LeafCount* [*eqR00*] = 17,408, *LeafCount* [*eqR11*] = 27,528, *LeafCount* [*eqR22*] = 134,929 for the first 3 equations. To verify the equations, the TOV equation was derived by symbolic manipulation for $\omega = 0$ $a = 0$ from *eqR00*, *eqR11*, *eqR22*, *eqR41*.

The power of Mathematica is sufficient to solve the TOV equation with the single procedure *NDSolve*. For the full Einstein equations it fails even for the ordinary differential equations (odeq) in *r*arising for fixed θ. It took us a long time to find an algorithm, which could handle the complexity of the equations and solve them in an acceptable time (3 - 5 minutes on a 16 × 8 lattice) on a PC-desktop and converge in the required region with an acceptable error of around 0.01.

For the second numerical stage we tried several slicing algorithms, and the best alternative proved to be the *θ-slicingr-forward* algorithm implemented by hand in Mathematica. The solution of the resulting odeq in each r-step was calculated using *NDSolve*.

Also, for every star model and parameter set, the TOV solution with $\omega = 0$ $a = 0$ was calculated first with the algorithm and compared with the exact TOV solution.

5. The TOV Equation as the Limit $\omega \to 0$ for the Extended Kerr Space-Time

In the Schwarzschild spacetime $\omega = 0$ and $a = 0$, we have spherical symmetry, no dependence on θ, then the TOV-equation can be derived from the remaining non-trivial Einstein equations eqR00, eqR11, eqR22, eqR41.

The TOV-equation is in the standard form:

$$P'(r) = -\left(\frac{GM(r)\rho(r)}{r^2}\right)\left(1+\frac{P(r)}{\rho(r)c^2}\right)\left(1+\frac{4\pi r^3 P(r)}{M(r)c^2}\right)\left(1-\frac{2GM(r)}{rc^2}\right)^{-1} \quad (13)$$

and using r_s

$$P'(r) = -\left(\frac{c^2 r_s \rho(r)}{2r^2}\right)\left(1+\frac{P(r)}{\rho(r)c^2}\right)\left(1+\frac{4\pi r^3 P(r)}{M(r)c^2}\right)\left(1-\frac{r_s M(r)}{rM_t}\right)^{-1},$$

where

M_t is the total mass, furthermore

$$4\pi r^2 \rho(r) = M(r), \quad P(r) = k_1 \rho(r)^{\gamma}$$

In order to make the variables dimensionless, one introduces "sun units"

$$r_{ss} = r_s(sun) = \frac{2GM_{sun}}{c^2} = 3\text{ km}, \rho_s = \frac{M_{sun}}{4\pi r_{ss}^3/3} = 1.76\times 10^{16}\frac{\text{g}}{\text{cm}^3}, P_s = \rho_s c^2$$

where r_{ss} Schwarzschild-radius of the sun, ρ_s the corresponding Schwarzschild-density and P_s the corresponding Schwarzschild-pressure.

In "sun units" TOV-equation transforms into

$$\begin{aligned} &P_1'(r_1) r_1^3 \left(r_1 - M_1(r_1) M_0\right) \\ &= -\frac{1}{2}\left(\frac{M_1'(r_1) M_0}{3} + P_1(r_1) r_1^2\right)\left(M_1(r_1) M_0 + 3P_1(r_1) r_1^3\right) \end{aligned} \quad (14)$$

with the normalized mass $M_1(r_1)$, and $M_1(R_1) = 1$, or

$$P_1'(r_1) r_1^3 \left(r_1 - M(r_1)\right) = -\frac{1}{2}\left(\frac{M'(r_1)}{3} + P_1(r_1) r_1^3\right)\left(M(r_1) + 3P_1(r_1) r_1^3\right)$$

where $M_0 = \frac{M_t}{M_{sun}}$, $M(r_1)$ is the mass within the radius r, $M(r_1) = M_0 M_1(r_1)$ in dimensionless variables r_1, $\rho(r_1) = \frac{M'(r_1)}{3r_1^2}$, M, $P_1 = k_1 \rho(r_1)^{\gamma}$ and R_1 is the dimensionless radius of the star.

With the replacement $P = k_1 \rho^{\gamma}$ for the pressure from the equation of state and $\rho = \frac{M_0 M'}{3r^2}$ we obtain a diff. equation for M degree 2 in r and we impose the boundary condition in $r = R_1$:

$M(R_1) = M_0$, $M'(R_1) = 0$ for non-interacting Fermi-gas and for an interacting Fermi-gas: $M(R_1) = M_0$, $M'(R_1) = \rho(R_1) 3R_1^2$, $\rho(R_1) = \rho_e$, where ρ_e is the equilibrium density in the minimum of V_{nn} and $P_1'(\rho_e) = 0$ (here an equivalent boundary condition is $\rho'(R_1) = \infty$).

6. The Equation of State and Rotation Parameters

6.1. The Equation of State for an (Non-Interacting) Nucleon Gas

Here, $P = k_1 \rho^{\gamma}$ is the equation of state of the star, derived from the thermodynamic Fermi gas equation at $T = 0$ ([1], chap. 48).

$$P = -\frac{\partial E}{\partial V} = 8\pi P_0 \left(\frac{x_F^3}{3}\sqrt{1+x_F^2} - f\left(x_F\right) \right) \tag{15}$$

$P_0 = \frac{mc^2}{\lambda_c^3} = \frac{m^4c^5}{h^3}$, where λ_c is the de-Broglie wavelength of the Fermi gas with particle mass m, $\lambda_c = \frac{h}{mc}$.

$x_F = \frac{p_F}{mc} = \frac{\lambda_c}{2}(3\pi)^{1/3} n^{1/3}$, where x_F is the Fermi-angular-momentum, n the particle density

$$f\left(x_F\right) = \int_0^{x_F} \mathrm{d}x\, x^2\sqrt{1+x^2}$$

The resulting approximate equations of state for P are

$$P = 8\pi P_0 \begin{pmatrix} \frac{x_F^5}{15} \\ \frac{x_F^4}{12} \end{pmatrix} = \begin{pmatrix} K_1\rho^{5/3} & \rho \ll \rho_c \\ K_2\rho^{4/3} & \rho \gg \rho_c \end{pmatrix} \tag{16}$$

valid for the density ρ and the critical density ρ_c

$$\rho_c = \frac{m}{\lambda_c^3}\frac{8\pi}{3}$$

The full expression for P, including temperature T, is as follows ([5], chap.15).

Here, we use dimensionless variables (r_1 distance unit de-Broglie-wavelength λ_c, V_1 volume unit λ_c^3, n_1 particle density unit $1/\lambda_c^3$, E_1 energy unit $E_0 = \frac{\hbar c}{\lambda_c} = \frac{mc^2}{2\pi}$, inverse thermal energy $\beta_1 = \frac{E_0}{kT}$, chem. potential μ_1 in E_0)., for the gas model we use the Debye model with the state density $D_1\left(E_1\right) = \frac{1}{4\pi^{7/2}}\sqrt{E_1}$, maximum energy $\varepsilon_{F1} = \frac{3^{2/3}\pi^{1/3}}{4} n_1^{2/3}$, the resulting particle density is

$$n_1 = \frac{N_{op}}{V_1} = \frac{2}{V_1}\int_0^\infty \mathrm{d}\omega_1 \frac{D_1\left(\omega_1\right)}{1+\exp\left(\beta_1\left(\omega_1-\mu_1\right)\right)}$$

$$= \frac{1}{2\pi^{7/2}}\int_0^\infty \mathrm{d}\omega_1 \frac{\sqrt{\omega_1}}{1+\exp\left(\beta_1\left(\omega_1-\mu_1\right)\right)}$$

From this relation the chem. potential μ_1 can be calculated, an approximation formula is

$$\mu_1 = \varepsilon_{F1} - \frac{\pi^2}{12\beta_1^2\varepsilon_{F1}} = \mu_1\left(n_1\right)$$

Finally, the resulting pressure (=energy density) $p_1\left(\beta_1, n_1\right)$:

$$p_1\left(\beta_1, n_1\right) = \frac{4\pi^{3/2}}{3\pi^2}\int_0^\infty \mathrm{d}\omega_1 \frac{\omega_1^{3/2}}{1+\exp\left(\beta_1\left(\omega_1-\mu_1\left(n_1\right)\right)\right)} \tag{17}$$

Below a 3D-diagram of $p_1\left(\beta_1, n_1\right)$ in dimensionless variables for a nucleon

gas ($m = m_n$, density $\rho = \frac{E_0 n}{c^2}$ in sun units, E_0 = 149.4 MeV) is depicted in Figure 1 [6].

Here kT is in E_0 units, and one sees the dependence $P = k_1 \rho^{\gamma}$ except on the left side, when kT reaches the magnitude of 1 Gev ($T = 10^{10}$K).

6.2. The Equation of State for an (Interacting) Nucleon Fluid

For the interacting nucleon gas we take into account the nucleon-nucleon-potential in the form of a Saxon-Woods-potential modeled on the experimental data: [7]-[13]

$$V_{sw}(r, V_0, r_0, d_{r0}) = \frac{V_0}{1 + \exp\left(\frac{r - r_0}{d_{r0}}\right)}$$

$$V_{nn}(r) = -V_{sw}(r_a, V_a, r_a, d_{ra}) + V_{sw}(r_c, V_c, r_c, d_{rc})$$

where V_{nn} is thenucleon-nucleon-potential with an attractive part $-V_{sw}(r_a, V_a, r_a, d_{ra})$ and a repulsive core $V_{sw}(r_c, V_c, r_c, d_{rc})$, the distance r between the nucleons is $r = (E_n/\rho)^{1/3}$, where $E_n = \left(m_n c^2/(2\pi)\right)^{1/3} = 149.4$ MeV $\approx m_\pi c^2$ is the nuclear energy scale m_π = pion mass = 140 MeV, m_n = neutron mass = 140 MeV.

The Saxon-Wood potential is shown in Figure 2 below.

The pressure of the interacting nucleon fluid becomes then

$$P_1(r_1) = c_1 \rho_1(r_1) V_{nn}\left((E_n/\rho_1(r_1))^{1/3}\right) \tag{18}$$

The experimental data used here are those from [7], and are shown in Figure 3.

And the hard-core potential from the lattice calculation Reid93 [10] is shown in Figure 4.

Both potentials are fitted with a double Saxon-Woods-potential V_{nn} in Figure 5:

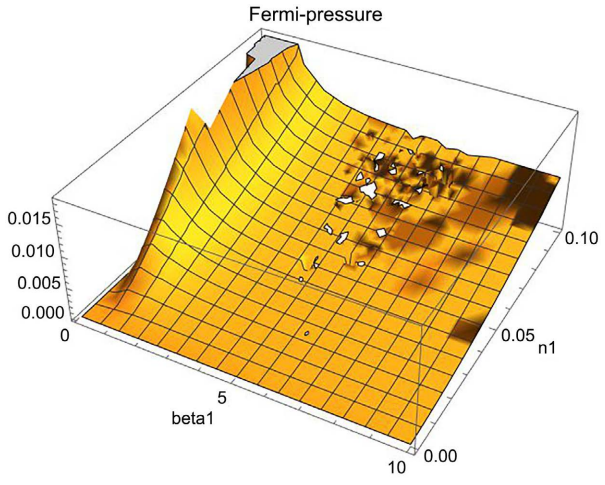

Figure 1. Fermi pressure.

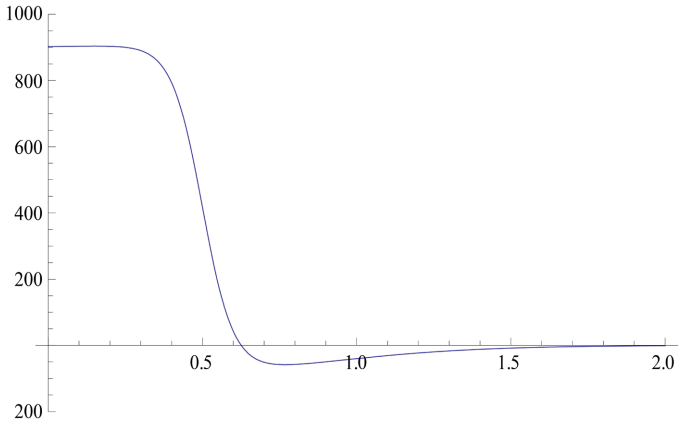

Figure 2. Saxon-Woodpotential $V_{nn}(r)$ with energy (MeV), r(fm) [6].

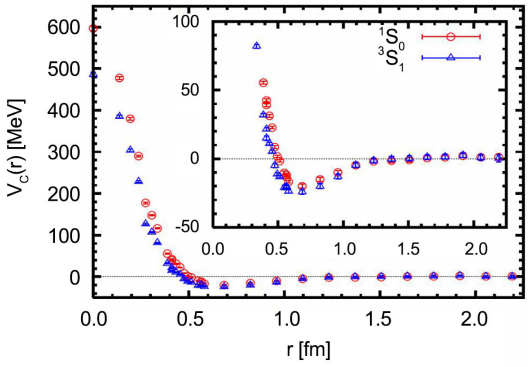

Figure 3. Nucleon-nucleon potential experimental data.

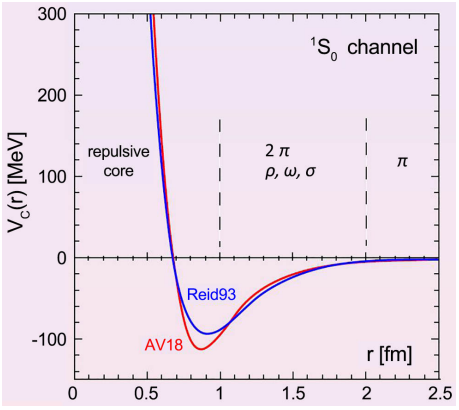

Figure 4. Nucleon-nucleon potential lattice calculation.

From the nucleon-nucleon-potential the pressure is calculated taking into account the low-density Fermi-pressure of the nucleons $P_{nf}(\rho)=K_1\rho^{5/3}$ and nucleon-nucleon pressure $P_{nn}(\rho)=V_{nn}\left(\rho^{-1/3}\right)\rho$ is shown in **Figure 6** [6], and the total pressure $P_{fg}(\rho)=K_1\rho^{5/3}+P_{nn}(\rho)$ is shown in **Figure 7**.

This equation-of-state has a minimum at $\rho=\rho_c=0.0417$ and $P'(r)=1$ at $\rho=\rho_m=0.0544$.

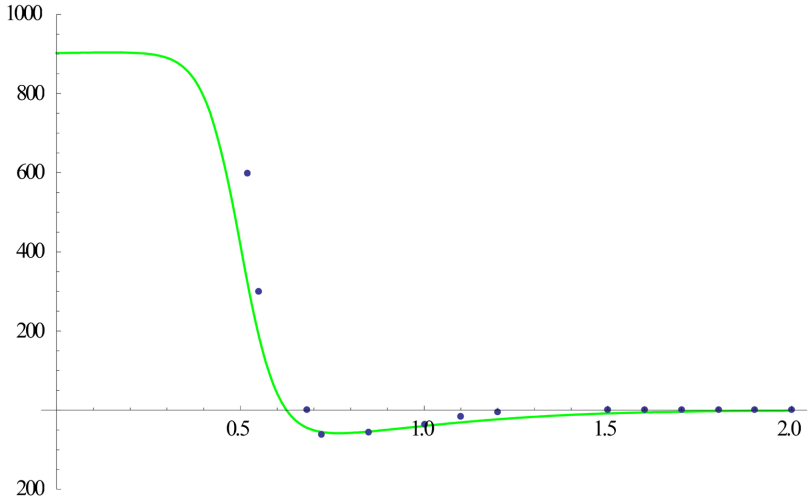

Figure 5. Nucleon-nucleon potential data fitted with Saxon-Wood-formula, with r(fm), V(MeV).

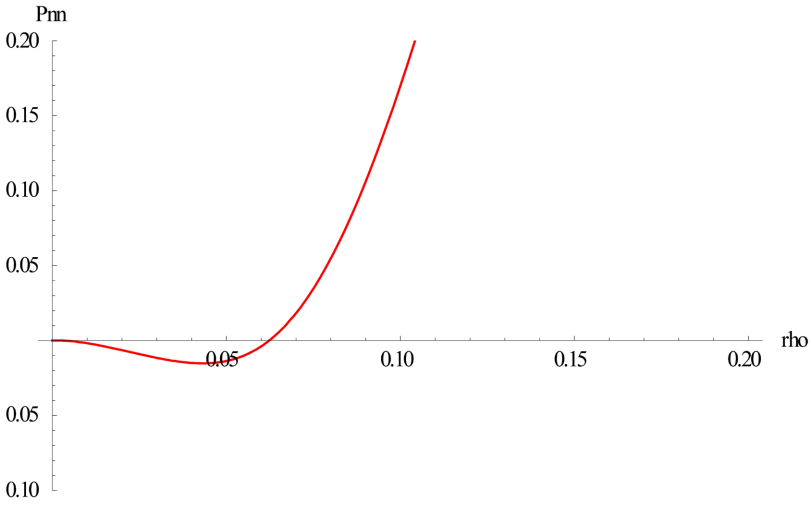

Figure 6. Nucleon-nucleon Fermi-pressure.

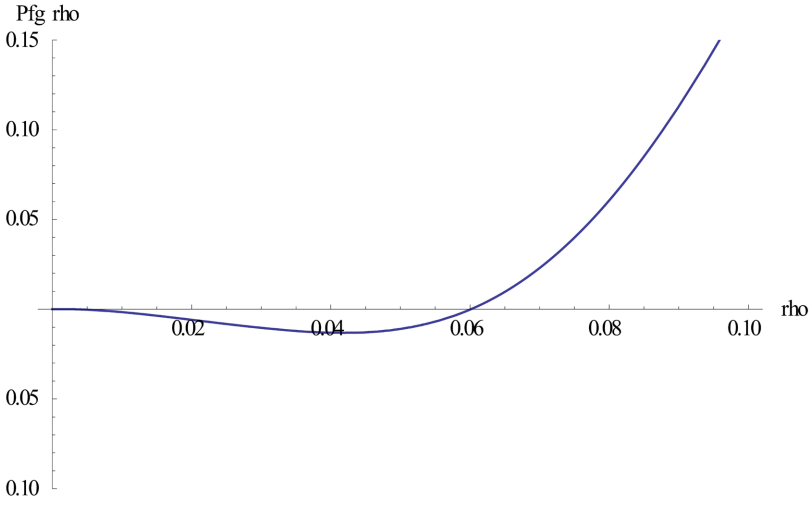

Figure 7. Total pressure $P_{fg}(r)$, pressure P and density r shown in sun-units.

As the sound velocity $v = \frac{dP(\rho)}{d\rho}$, $v > 0$ and $v < 1$ (*i.e.* subluminal), the admissible density range in the neutron-fluid model is $\rho_c \le \rho \le \rho_m$.

6.3. Maximum Omega-Values in Kerr-Space-Time

We consider here a rotation model with constant angular velocity ω. With this model the resulting 4-velocity u^μ has the form [4] [14] [15]:

$$u^\mu = \left(u^0, 0, 0, \omega u^0\right)$$

The maximum values for ω are calculated from the minimal zeros in omega of the denominator in u^0 from (9a), minimized over r_1 and *th* in their respective regions

$$r_i \le r_1 \le R_1 \quad \text{and} \quad 0 \le \theta \le \pi/2.$$

The resulting value is $\omega \le \frac{1}{2R_1\sqrt{\alpha_f}}$, where α_f is the form-factor in the moment of inertia I_1.

$I_1 = \alpha_f M R_1^2$, α_f = 2/3 for a shell, α_f = 2/5 for a sphere.

With non-vanishing density the actual $\omega_{\max}$ depends on $\{Ai, \rho\}$, and has to be calculated from the above expression for u^0.

A less stringent limit for omega can be deduced from the limit for the parameter a in Kerr-spacetime (in sun-units and c = 1): $a \le \frac{r_s(M_0)}{2} = \frac{M_0}{2}$, and $a = \frac{\alpha_f M_0 R_1^2 \omega}{M_0}$ therefore $\omega \le \frac{M_0}{2R_1^2\alpha_f}$

7. The TOV-Equation: A New Ansatz

Generally speaking, the parameters of the solution are (in brackets denomination in program code): angular momentum radius a (=alpha1, =0 for TOV), the factor in the state equation k_1, the power in the state equation γ (=gam), radius R, mass M_0, the relative radius uncertainty $dr02_{rel}$ (=dr02rel), the moment of inertia factor f_I (= infac, 0 for TOV), the singularity smoothing parameter ε (=epsi, see below), and the boundary factor n_{rmax} (=nrmax). Here the boundary factor enters the upper boundary of the TOV differential equation as $r_{max} = R\left(1 + n_{rmax} dr02_{rel}\right)$.

The dimensionless TOV-equation is a differential equation in the mass $M(r)$ of degree 2, and is highly non-linear, the dimensionless mass-density relation is $\rho = \frac{M'}{3r^2}$.

The customary way of solving the TOV equation is to impose the boundary condition at r = 0 with $M(0)$ = 0, $M'(0) = 3r^2\rho_0$ where ρ_0 the maximum central density.

In the new ansatz for the mass $M(r)$ we impose the *outer* boundary condition at $r = R_1$:

for a pure Fermi-gas without interaction: $M(R_1) = M_0$, $M'(R_1) = \rho(R_1)3R_1^2$, $\rho(R_1) = 0$;

for an interacting Fermi-gas: $M(R_1) = M_0$, $M(R_1) = \rho(R_1)3R_1^2$, $\rho(R_1) = \rho_e$, where ρ_e is the equilibrium density in the minimum of V_{nn} and $P_1'(\rho_e) = 0$ (here an equivalent boundary condition is $\rho'(R_1) = \infty$).

The star parameters mass M_0 and radius R_1, which enter the outer boundary condition determine completely the solution. In general, there will be an *inner radius* $r_i > 0$ with the maximum density $\rho_0 = 3r^2M'(r_i)$ and $M(r_i) = 0$. The corresponding "dual" parameters are the inner radius r_i and the maximum density ρ_0. One can show that for $\rho_0 \gg \rho_c$ (where ρ_c is the critical density of the equation of state) there is no solution with a compact star $r_i = 0$, *i.e.* there is a maximum mass M_c for the TOV equation, in case of compact neutron stars $M_c = 3.04M_{sun}$ (see below). As we will see, there is in general a solution, if we allow $r_i > 0$ and impose an outer boundary condition at $r = R_1$, as long as R_1 is not too close to the Schwarzschild radius $r_s = M_0$ of the star. In the limit $R_1 \to r_s$ there will be no positive zero of $M(r)$, *i.e.* $r_i < 0$ and the resulting (mathematical) TOV-solution will be no physical solution. But in general, speaking naively, the gravitational collapse of the star is avoided for large masses ($M_0 > M_c$), if it has a shell structure with the inner radius r_i and the outer radius $R_1 > M_0$.

As we will see, this outer boundary condition together with allowing $r_i > 0$ changes dramatically the resulting manifold of physical solutions.

7.1. The TOV-Equation: The Parametric Solution and Resulting Star Types

By setting-up a parametric solution of the TOV-equation one gets *a map of possible physical solutions*, *i.e.* possible star structures. As parameters one can use either (M_0, R_1) in the outer boundary condition at $r_1 = R_1$ or the *dual* parameter pair (r_i, ρ_{bc}) in the inner boundary condition $r_1 = r_i$.

The pure neutron Fermi-gas model yields for compact neutron stars a maximum mass of $M_{maxc} = 0.93M_{sun}$, which is in disagreement with observations. Therefore, at least for compact neutron stars, a model of interacting neutron fluid must be used. In 6.2 above we have described a Saxon-Wood-potential model for the nucleon-nucleon interaction, which seems to fit the experiment and the theory in the best way. There will be a critical density (dependent on temperature of course), where a transition from interacting fluid to Fermi-gas takes place, it is plausible to set this density equal to the Saxon-Wood critical density

$$\rho_c = 0.0417 .$$

We made calculations with the TOV-equation using these two models for neutron-based stars and we came to the conclusion that compact neutron stars with mass $M_0 \leq 3.04M_{sun}$ consist of interacting neutron fluid and neutron shell-stars for $M_0 \geq 5M_{sun}$ obey the Fermi-gas model. The underlying calculation is the Mathematica-notebook [6].

This approach yield results, which are described below.

Neutron stars consist of *interacting neutron fluid* and are compact stars with $(M_0, R_1) = (0.14, 1.49), \ldots, (3.04, 3.95)$ and the maximum density $0.048 \le \rho_{bc} \le 0.0544 = \rho_{bcmax}$ in sun-units, or shell-stars with $\rho_{bc} \ge \rho_{bcmax}$ and $(M_0, R_1) = (3.04, 3.95), \ldots, (4.91, 4.92)$, neutron star *R-M*-relation follows approximately a cubic-root-law: $R \sim M^{1/3}$.

Stellar shell-stars consist of (almost) *non-interacting Fermi-gasof neutrons* and are *thin shell-stars* with $R_1 > r_s$, $R_1 \approx r_s$, $r_i \approx r_s$, *i.e.* the shell is close to the Schwarzschild-radius and its outer edge outside the Schwarzschild-horizon with max. density $0.0025 \le \rho_{bc} \le 0.042$, and obey an almost linear R-M-relation $(M_0, R_1) = (5.5, 9.1), \ldots, (81.3, 91.2)$, independent of ρ_{bc} for $\rho_{bc} \ge 0.028$, with redshift factor around 50 for $M = 80 M_{sun}$.

Galactic (supermassive) shell-stars are *very thin shell-stars*, which obey the *equation-of-state of a white-dwarf* (*i.e.* gravitation counterbalanced by Fermi-pressure of electron gas) and have an almost linear R-M-relation with redshift factor 20…100.

Neutron stars

The parametric solution of the TOV-equation has been carried out for the parameters (ρ_{bc}, r_i) at the boundary $r = r_i$, in the range: density $0.02 \le \rho_{bc} \le 0.15$ and inner radius $0.01 \le r_i \le 15$, yielding physical solutions for density $0.048 \le \rho_{bc} \le 0.0544 = \rho_{bcmax}$ andinner radius $0.01 \le r_i \le 3$. The TOV-equation is solved for $M(r)$ and $\rho(r)$, and a physical solution is a mathematical solution with $M \ge 0$ and $\rho \ge 0$, $\rho' \le 0$ and subluminal equation-of-state within a certain interval $r = \{r_i, r_{02}\}$, which reaches a point, where $M'(r) = 0$ and $\rho(r) = 0$. The radius R_1 and the total mass M_0 is reached at $M'(R_1) = 0$, the physical solution ends there.

The validity interval for ρ is explained by the fact, that the sound velocity $v_s(\rho) = \dfrac{\partial P(\rho)}{\partial \rho}$ must be positive and below 1 (subluminal in c-units).

The parametric mapping of the solutions results in the following dependence for $M_0(r_i, \rho_{bc})$, $R_1(r_i, \rho_{bc})$ $(r_i, \rho_{bc}, M_0, R_1$ insun-units) (**Figure 8** [6]):

For $r_i = 0$ the mapping describes the compact neutron stars, resulting in $R_1(M_0)$ function (**Figure 9(a)**, **Figure 9(b)**, **Figure 10** [6]):

The *R-M*-relation follows approximately a cubic-root-law: $R \sim M^{1/3}$, with a range of $(M_0, R_1) = (0.14, 1.49), \ldots, (3.04, 3.95)$, *i.e.* the resulting maximum compact mass is $M_{maxc} = 3.04\ M_{sun}$.

For $M_0 \ge M_{maxc}$ the function $R_1(r_i = const, \rho_{bc})$ is flat or slightly decreasing with ρ_{bc}, so one expects the stable configuration to be the one with maximum $\rho_{bc} = \rho_{bcmax}$, with a range of $(M_0, R_1) = (3.04, 3.95), \ldots, (4.91, 4.92)$.

The admissible mass range ends, where the thickness of the shell above the Schwarzschild-radius becomes very small (minimum 0.01).

So in total the *R-M*-relation for neutron stars becomes

The maximum mass for a repulsive-hardcore-model for the equation-of-state DD2 [16] is $2.42 M_{sun}$, from our mapping we have the maximum compact neutron star mass of $M_{maxc} = 3.04 M_{sun}$.

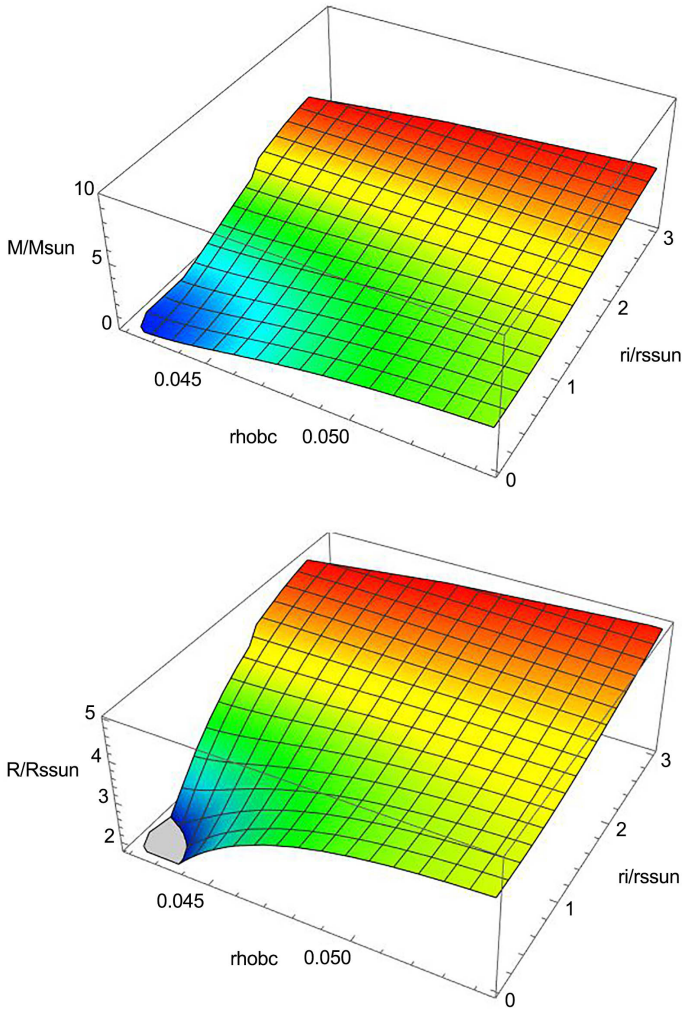

Figure 8. Neutron star: mass M and radius R in dependence of inner boundary density ρ_{bc} and inner radius r_i.

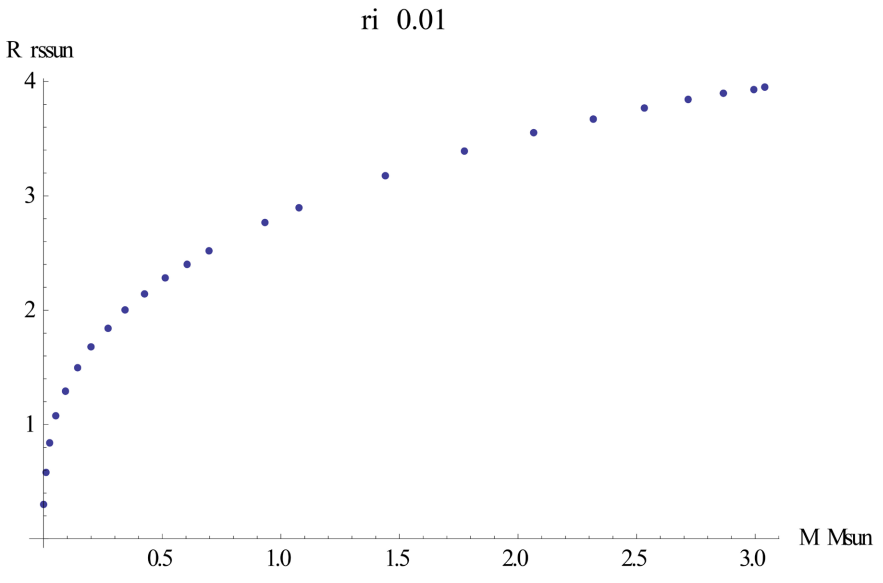

(a)

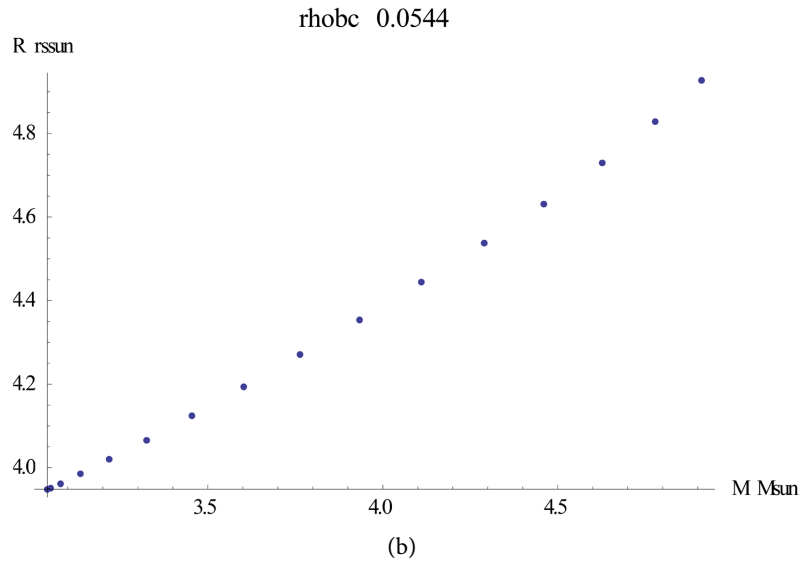

Figure 9. (a) Compact neutron star: mass-radius *R-M* relation; (b) Shell neutron star: mass-radius *R-M* relation.

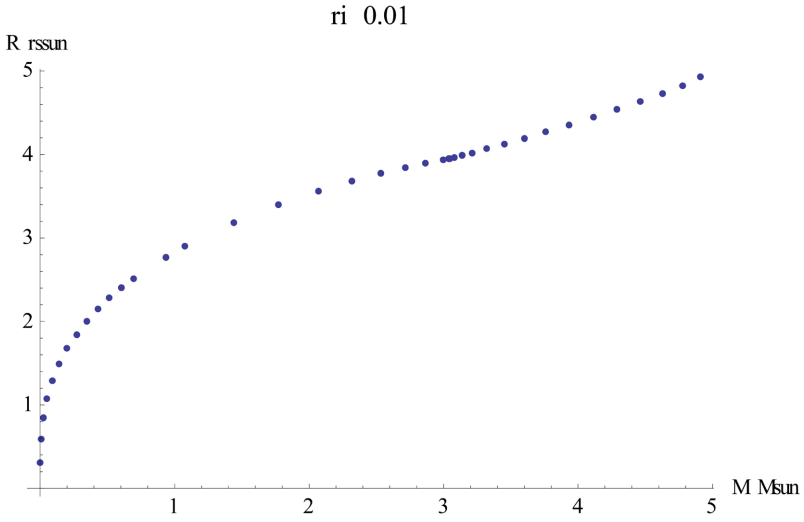

Figure 10. Neutron star: mass-radius *R-M* relation.

The actual theoretical limit for neutron star core density is $\rho_{max} = 3.5 \times 10^{15}$ g/cm^3 = 0.199 in sun-units [8] [9].

The limit for ρ_{bc} reached in our mapping is only ¼ of this $\rho_{bc} = \rho_{bcmax} = 0.0544$, due to the subluminal-sound-condition and the use of an (attractive) nucleon-nucleon-potential for the nucleon-fluid instead of a pure repulsive-hardcore-model.

The classical argument for the collapse of a neutron star to a black-hole for $\rho_{bc} > \rho_{max}$, dating back to Oppenheimer [1], is invalidated here by the simple introduction of shell-star models, where $r_i > 0$, and therefore there is no mass at the center, which means physically, there is only a very diluted nucleon gas there.

Stellar shell-stars (stellar black-holes)

We assume that the underlying equation-of-state state for stellar shell-stars is the Fermi-gas of nucleons with the low-density limit of

$$P(\rho) = K_1 \rho^{5/3}.$$

We make a further plausible assumption that the "edge" of the solution mapping are the physically stable solutions, *i.e.* the R-M-relation for stellar shell-stars. The edge in this case consists for fixed $\rho_{bc} < 0.0417 = \rho_{oc}$ of solutions with maximum r_i (because then the average density in the shell is lowest) and for $\rho_{bc} = 0.0417 = \rho_{oc}$ it consists of the solutions (M_0, r_i, R_1) at the right boundary ($7 \leq r_i \leq 22$, $M_0 \geq 4.91 = M_{maxn}$), where M_{maxn} is the maximum mass for the neutron star interactive neutron fluid. We assume that at $\rho_{bc} = \rho_{oc}$ the state transition from the interactive neutron fluid to neutron Fermi gas takes place. This is almost certainly an oversimplification, still we believe that the model describes the reality correctly in principle.

The chosen parameter range of the solution mapping is: density $0.025 \leq \rho_{bc} \leq 0.0417 = \rho_{oc}$ and inner radius $0.01 \leq r_i \leq 90$, where ρ_{oc} is equilibrium value of the nucleon-nucleon-potentials with $\mathrm{Pnf}'(\rho_{oc}) = 0$, the transition point from the nucleon-fluid to the nucleon-gas phase.

The "edge" of the mapping yields the (M_0-, r_i, R_1-)-range of $(M_0, r_i, R_1) = (5.35, 7, 8.49), \ldots, (81.3, 89.6, 91.2)$, where the upper limit is in fact mathematically open, but the "thinning-out" of the solutions for small ρ_{bc} and large r_i makes it physically plausible (see **Figure 11** [6] below).

The resulting *R-M*-relation is practically linear and has a maximum mass value of $M_{max} = 81.3 M_{sun}$. (**Figure 12(a)**).

And the corresponding relative shell thickness $dR_{rel} = dR/M$ is (**Figure 12(b)**) and the relative Schwarzschild-distance $dR_{srel} = (R - M)/M$ is (**Figure 13**)

The inverse of dR_{srel} gives roughly the light attenuation factor of {1.7, …, 20.}. Taken the attenuation factor and the small relative shell thickness of around 0.02, these stellar shell-stars have approximately the properties expected of a genuine black-hole, when measured from a distance $r \gg R_1$.

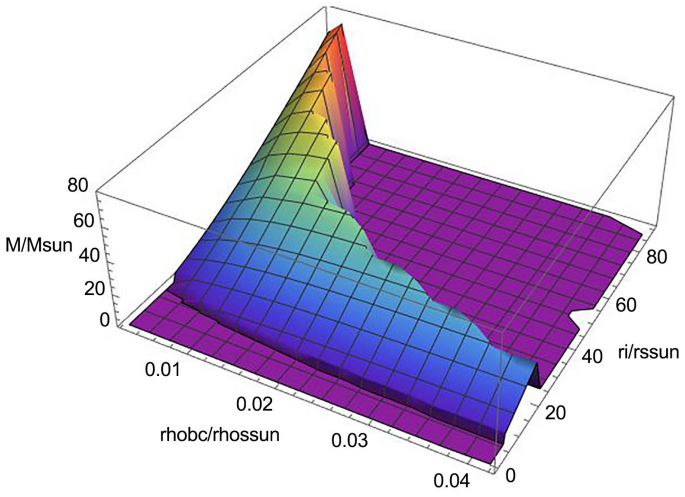

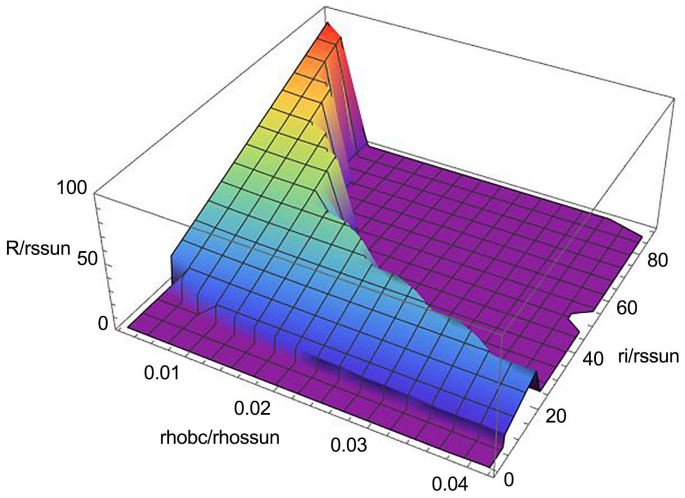

Figure 11. Stellar shell star: mass M and radius R in dependence of inner boundary density ρ_{bc} and inner radius r_i.

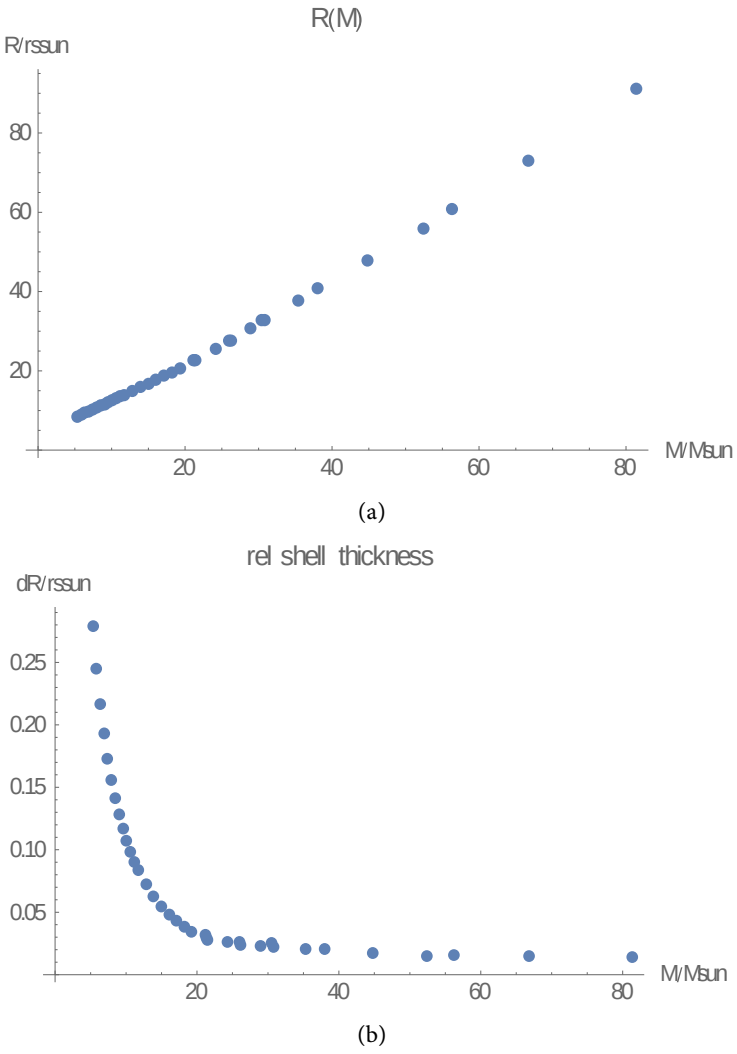

Figure 12. (a) Stellar shell star: mass-radius R-M relation; (b) Stellar shell star: relative shell thickness.

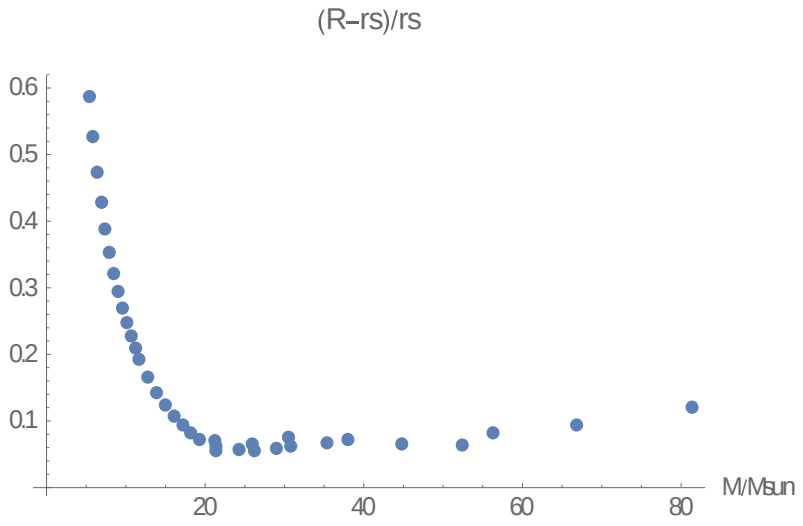

Figure 13. Stellar shell star: relative Schwarzschild-distance.

Entropy of a thin shell star

The celebrated Bekenstein-Hawking formula for the entropy of a black hole reads [17]:

$S = \frac{k_B A}{4L_P^2}$, where A is the surface area, k_B the Boltzmann-constant, and L_P the Planck-length.

The entropy of a (cold) shell-star with radius R and thickness dR in the limit $R = r_s$, $dR \ll r_s$, with all particles in the lowest possible energy state, can be easily calculated from the Boltzmann-formula

$S = k_B \ln W$, where W is the number of possible micro-states.

With the elementary area πL_{min}^2, where $L_{min} = L_P$, W becomes $W = 2^{A/\left(\pi L_{min}^2\right)}$ (each of the $N = A/\left(\pi L_{min}^2\right)$ area elements can be occupied or empty), so $S = \frac{k_B A}{\pi L_P^2}\ln 2$, which is identical to the Bekenstein-Hawking entropy with the factor $(\ln 2)4/\pi = 0.882$.

Galactic (supermassive) shell-stars

The mean density of a black-hole scales with its radius R like

$$\rho(R) = \frac{M}{V} = \frac{R}{(4/3)\pi R^3} = \frac{3}{4\pi R^2}$$

i.e. for supermassive black-hole with $M = 10^6 M_{sun}$ we have $\rho \approx 10^{-12}$ in sun units (su).

In the following we use the abbreviation $MM_{sun} = 10^6 M_{sun}$.

The density scale of a white-dwarf star is 10^6 g/cm^3 = 5.7 × 10^{-11} su [1]. Therefore it is plausible to try a parametric mapping with the white-dwarf equation-of-state, where the underlying Fermi-pressure is that of an electron gas instead of a nucleon gas, *i.e.* equation-of-state $P_1(r_1) = k_1 \rho_1(r_1)^\gamma$ for a pure Fermi gas, $\gamma = 5/3$ if the density is below the critical density ρ_c.

The results for $M_0(r_1, \rho_{bc})$, $R_1(r_1, \rho_{bc})$ are shown below (**Figure 14** [6]):

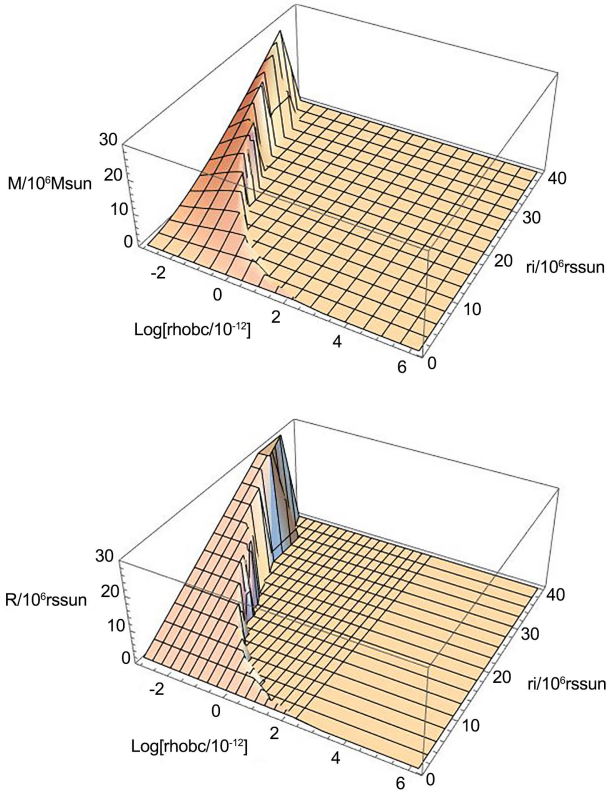

Figure 14. Galactic shell star: mass M and radius R in dependence of inner boundary density ρ_{bc} and inner radius r_i.

From this result one can draw several consequences: first, the actual density is around 10^{-12}, that is well below the critical density for a white-dwarf of $\rho_c = 0.91 \times 10^6$ g/cm^3 = 5.17×10^{-11} su: $\gamma = 5/3$ in the equation-of-state is justified. Second, the viable solutions lie to the left of a "ridge" reaching up to masses around 30 MM_{sun}. Third, a stable solution for a fixed mass will have the highest possible maximum density ρ_{bc} and that will lie on the "ridge". So one can calculate the R-M-relation following the "ridge".

The resulting R-M-relation is as follows (**Figure 15**).

And the inner radius is (**Figure 16**).

The R-M-relation is almost linear, as expected, and goes up to $50MM_{sun}$. $dR_{rel} = \left(R_1 - r_i\right)/M_0$ is the relative thickness (**Figure 17**), and shows, that the shells are very thin indeed, with a minimum of 0.001. The fourth diagram shows the relative Schwarzschild-distance (**Figure 18**) $dR_{srel} = \left(R_1 - M_0\right)/M_0$, which has a minimum at $\{M_0, dR_{srel}\} = \{7, 0.00142857\}$, so that its reciprocal value (approximate light attenuation factor) is around 700. So the overall result is, that the supermassive shell-stars become ever thinner shells, while the distance from the Schwarzschild-horizon is increasing.

7.2. The TOV-Equation: A Case Study for Typical Star Types

In the nearly-rotation-free case the solution of the TOV-equation was calculated for 4 models in sun units with r_s = Schwarzschild radius

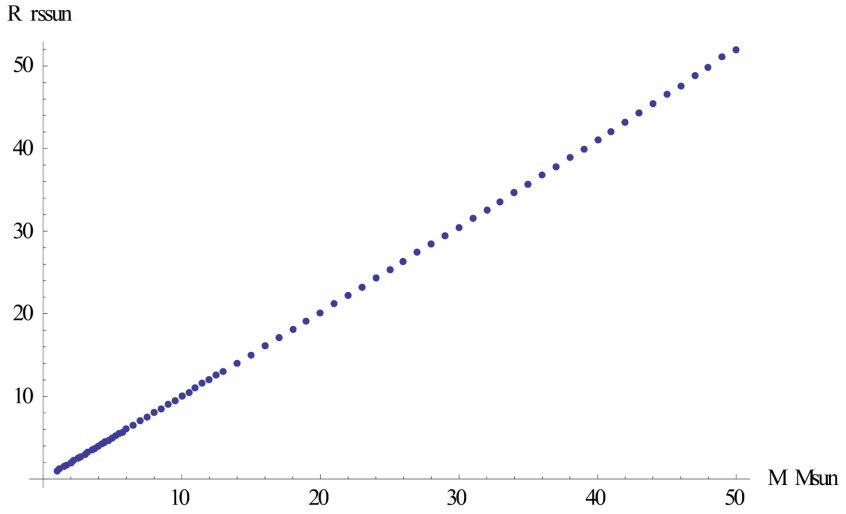

Figure 15. Galactic shell star: *R*-*M*-relation.

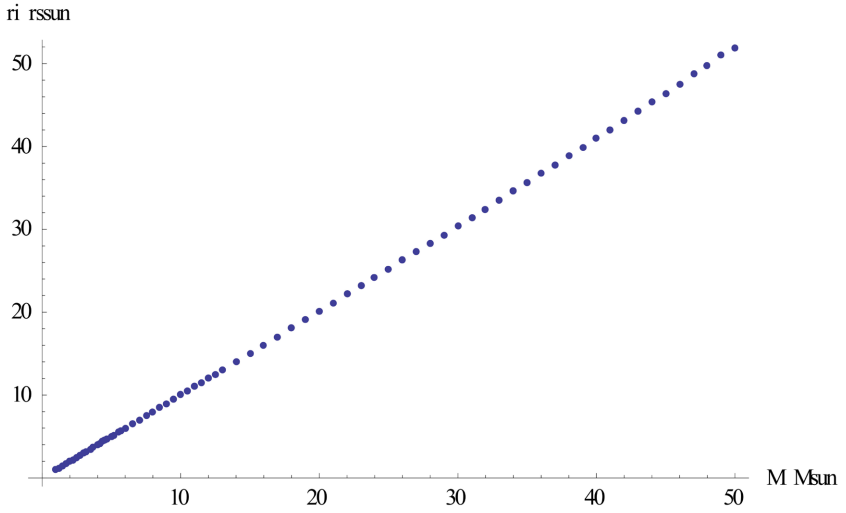

Figure 16. Galactic shell star: inner radius.

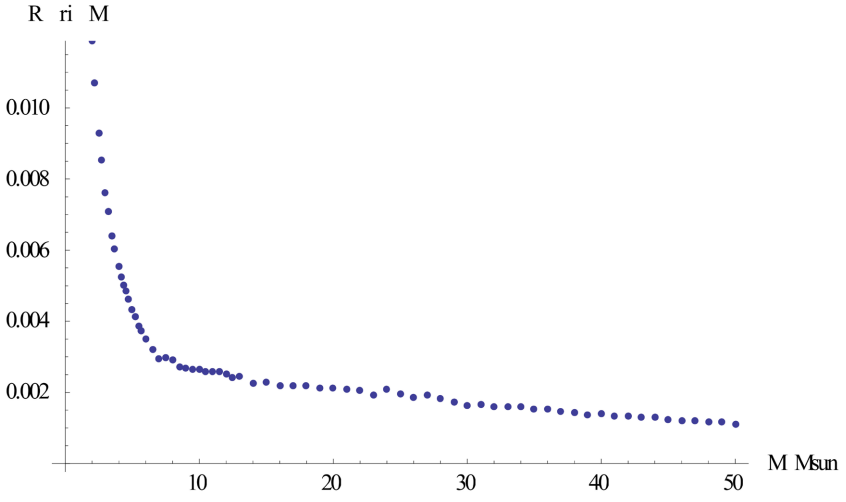

Figure 17. Galactic shell star: relative shell thickness.

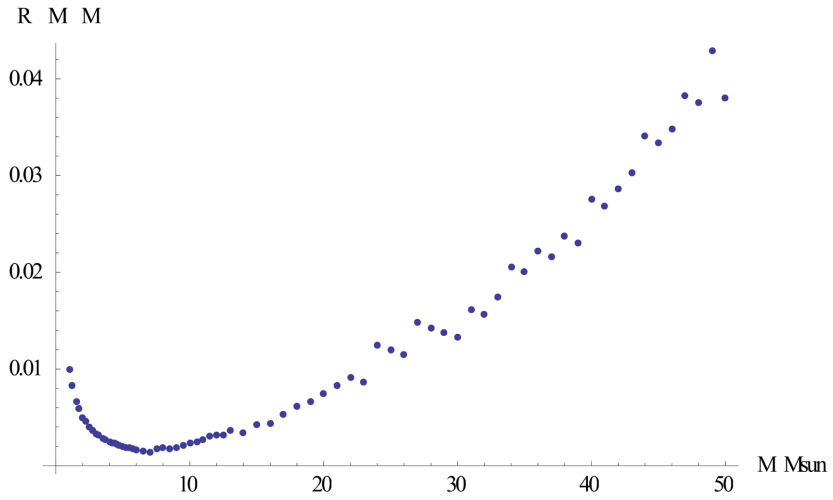

Figure 18. Galactic shell star: relative Schwarzschild distance.

$$r_{ss} = r_s(sun) = \frac{2GM_{sun}}{c^2},\quad \rho_s = \frac{M_{sun}}{4\pi r^3/3},\quad P_s = \rho_s c^2,$$

$$r_{ss} = 3\,\text{km},\quad \rho_s = 1.76\times 10^{16}\,\text{g/cm}^3,\quad M_{sun} = 3\times 10^{30}\,\text{kg},$$

- average compact neutron star with mass $M_0 = 0.932 M_{sun}$, radius $R_1 = 2.767 r_{ss}$.
- maximum mass neutron shell-star $M_0 = 4.91$, $R = 4.926$.
- white dwarf with $M_0 = 0.6 M_{sun}$, radius $R_1 = 3000 r_{ss}$.
- stellar black hole with $M_0 = 15.69 M_{sun}$, radius $R_1 = 17.89 r_{ss}$, inner radius $r_i = 17 r_{ss}$.
- galactic black hole with $M_0 = 4.367 \times 10^6 M_{sun}$, $R_1 = 4.380 \times 10^6 r_{ss}$, $r_i = 4.356 \times 10^6 r_{ss}$.

Compact neutron star

parameters = {k1 = 0.40, gam = 5/3, M0 = 0.932, R1 = 2.76, rhobc = 0.0456, ri = 0.01};

The mean density is here $\rho_{mean} = \frac{M_0}{R_1^3} = 0.04447$.

The critical density of the neutron Fermi gas with neutron mass m_n is $\rho_{cn} = \frac{m_n^4 c^3}{3\pi^2\hbar^3} = 0.35$ (see [17]), so the low-density approximation with $\gamma = 5/3$ can be used.

Results TOV:

density rho (**Figure 19**), mass M (**Figure 20**) are

As can be seen in the ρ-diagram, the derivative $\rho'(R_1) = \infty$, because there the equilibrium density ρ_c with $P'(r_c) = 0$ in the pressure is reached.

Maximum mass neutron shell-star

parameters = {k1 = 0.40, gam = 5/3, M0 = 4.91, R1 = 4.926, rhobc = 0.0544, ri = 3};

The mean density is here $\rho_{mean} = 0.0530$.

Results TOV:

density rho (**Figure 21**), mass M (**Figure 22**) is

Stellar shell-star (stellar black hole)

parameters = {k1 = 0.40, gam = 5/3, M0 = 15.69, R1 = 17.89, rhobc = 0.0359, ri = 17};

The mean density is here $\rho_{mean} = 0.0194$.

The resulting rho (Figure 23) and M (Figure 24) are:

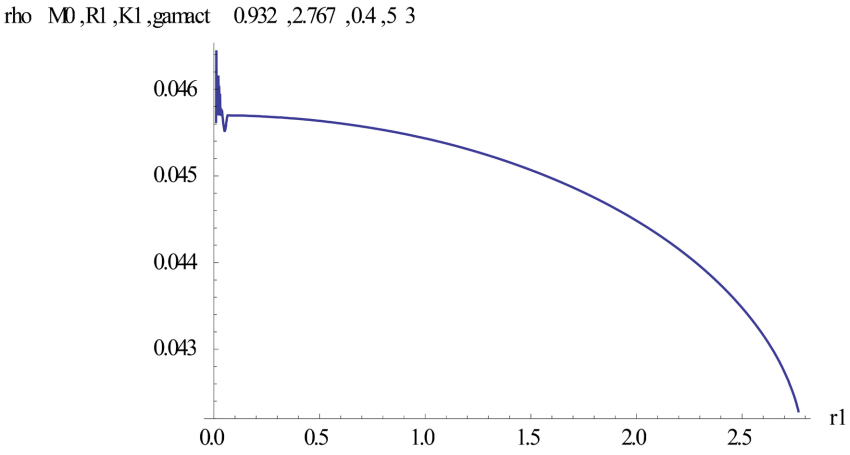

Figure 19. Typical compact neutron star: density in dependence of radius.

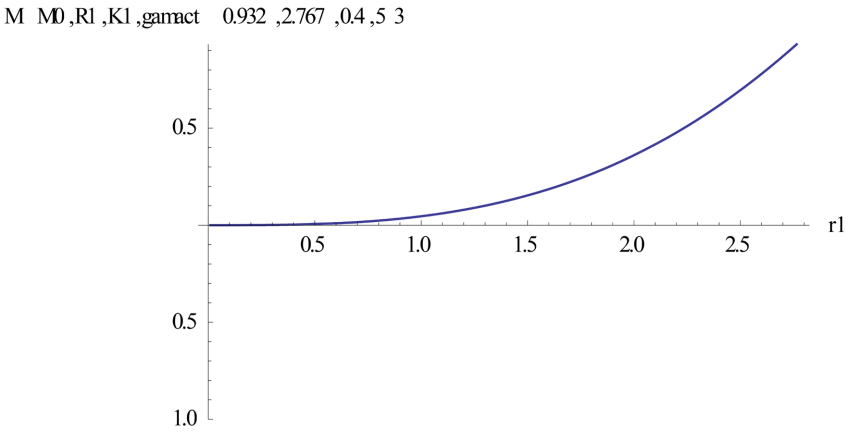

Figure 20. Typical compact neutron star: mass in dependence of radius.

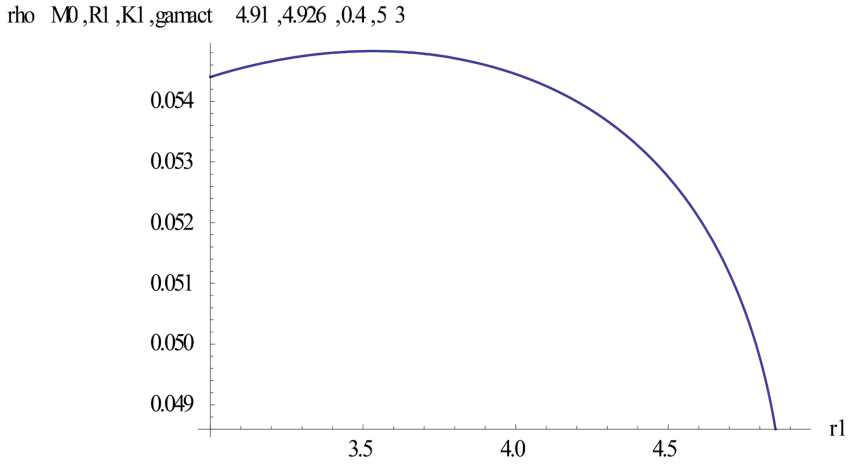

Figure 21. Shell neutron star: density in dependence of radius.

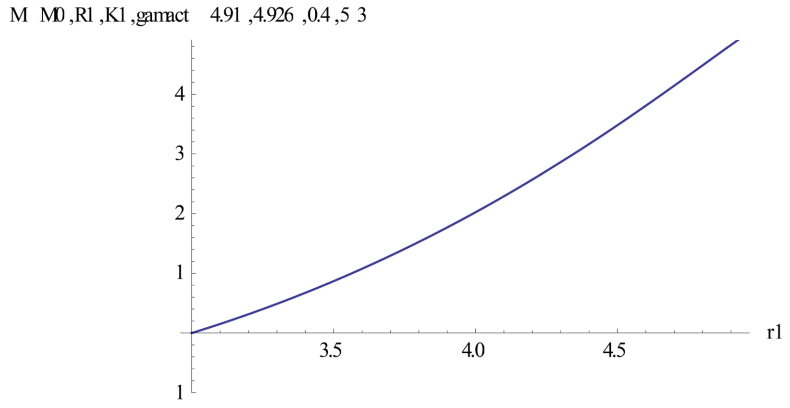

Figure 22. Shell neutron star: mass in dependence of radius.

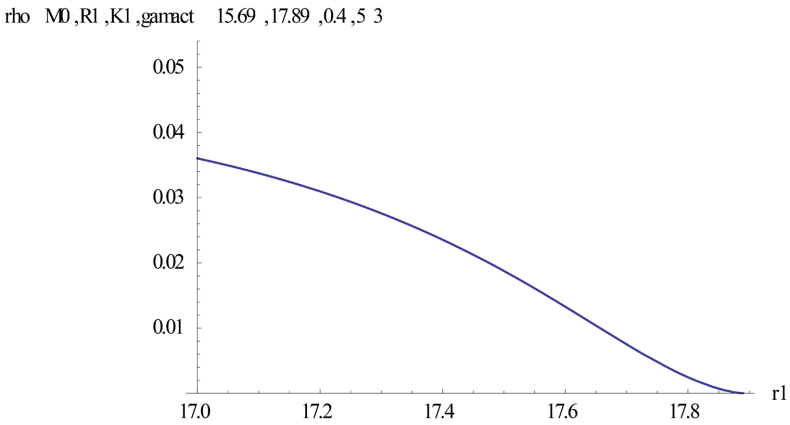

Figure 23. Typical stellar shell star: density in dependence of radius.

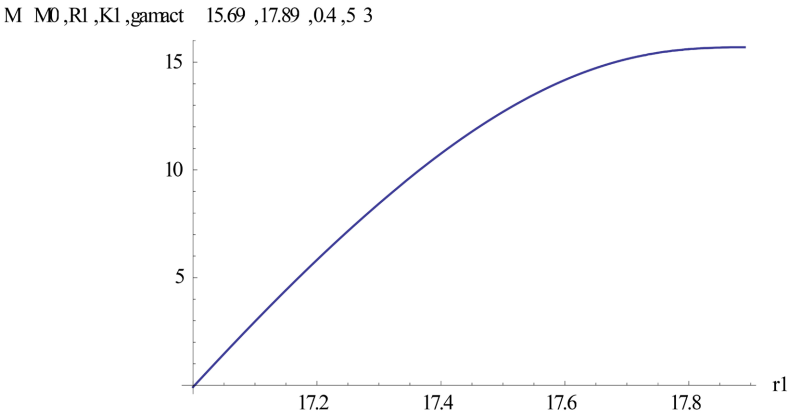

Figure 24. Typical stellar shell star: mass in dependence of radius.

Here the radius R_1 is reached, when $M(r_1 = R_1) = 0$, *i.e.* $\rho(R_1) = 0$.

White-dwarf star

parameters = {k1 = 1.43×10^6, gam = 5/3, M0 = 0.6, R1 = 3000, rhobc = 2.02×10^{-11}, ri = 0};

The underlying state equation is that of a small-momentum electron Fermi-gas with the critical density [1] $\rho_{cw} = \dfrac{m_e m_n^3 c^3}{3\pi^2 \hbar^3} = 0.517 \times 10^{-10}$ su .

The mean density is here $\rho_{mean} = 2.22 \times 10^{-11}$, the maximum deviation of ρ is $\Delta_{max}\rho = 0.21 \times 10^{-11}$, so the density is practically constant, as expected.

The solution of the TOV-equation yields density rho (Figure 25), mass M (Figure 26).

Galactic shell-star (supermassive black-hole)

parameters = {k11(γ = 5/3) = 0.0243×10^6, k12(γ = 4/3) = 0.067×10^4, M0 = 4.367×10^6, R1 = 4.380×10^6, rhobc = 4.934×10^{-12}, ri = 4.356×10^6};

TOV equation was solved with an exterior boundary condition $r_{02} = R_1$ ($M(r_{02}) = M_0$, $M(r_{02}) = 0$), which is equivalent to the interior boundary condition $r_{01} = r_i$ ($M(r_{01}) = 0$, $\rho(r_{01}) = \rho_{bc}$), and with the full Fermi-gas equation-of-state instead of the simple power law $P(\rho) = K_1\rho^{\gamma}$.

The mean density is here $\rho_{mean} = 3.16 \times 10^{-12}$.

The "naive" mean density is here $\rho_{mean} = \dfrac{M_0}{R_1^3} = 3.16 \times 10^{-12}$, *i.e.* by a factor 10 lower than the mean density of white dwarf. Therefore, despite its huge mass, the galactic black hole can be described by the state equation of a small-momentum (undercritical) Fermi electron gas with the relative density $x_F = \dfrac{\rho}{\rho_{cn}} = 0.0612$ much smaller than that for the white dwarf.

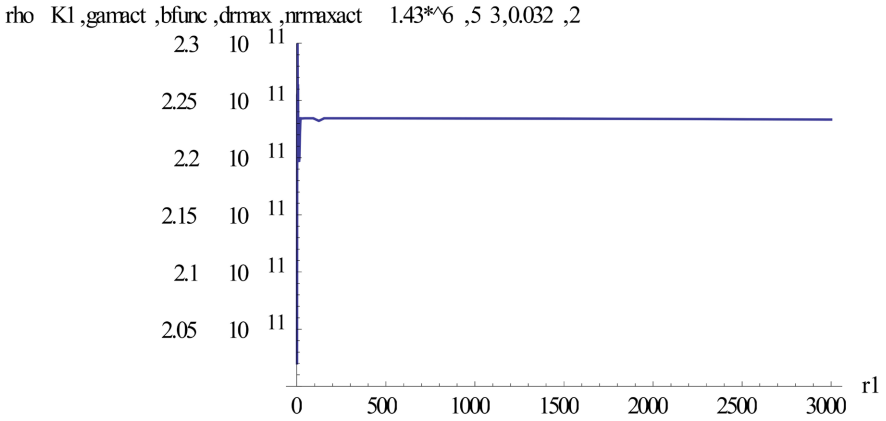

Figure 25. Typical white dwarf star: density in dependence of radius.

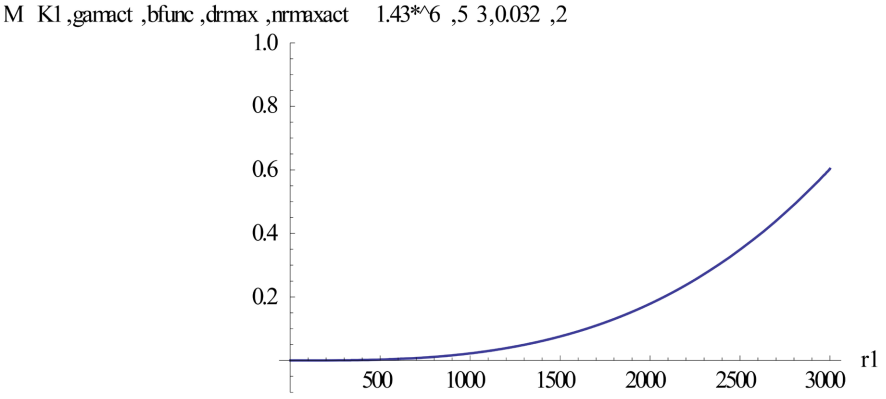

Figure 26. Typical white dwarf star: mass in dependence of radius.

TOV-solution for rho (in 10^{-12} units, Figure 27), M (in 10^6 units, Figure 28) in r (in 10^6 units), is:

Here there is an internal "hole" with a radius $r_i = 4.356 \times 10^6$, maximum $\rho = 4.934 \times 10^{-12}$ at r_i. The inner radius r_i lies a little below the Schwarzschild-radius $r_s = M_0$. The relative shell thickness

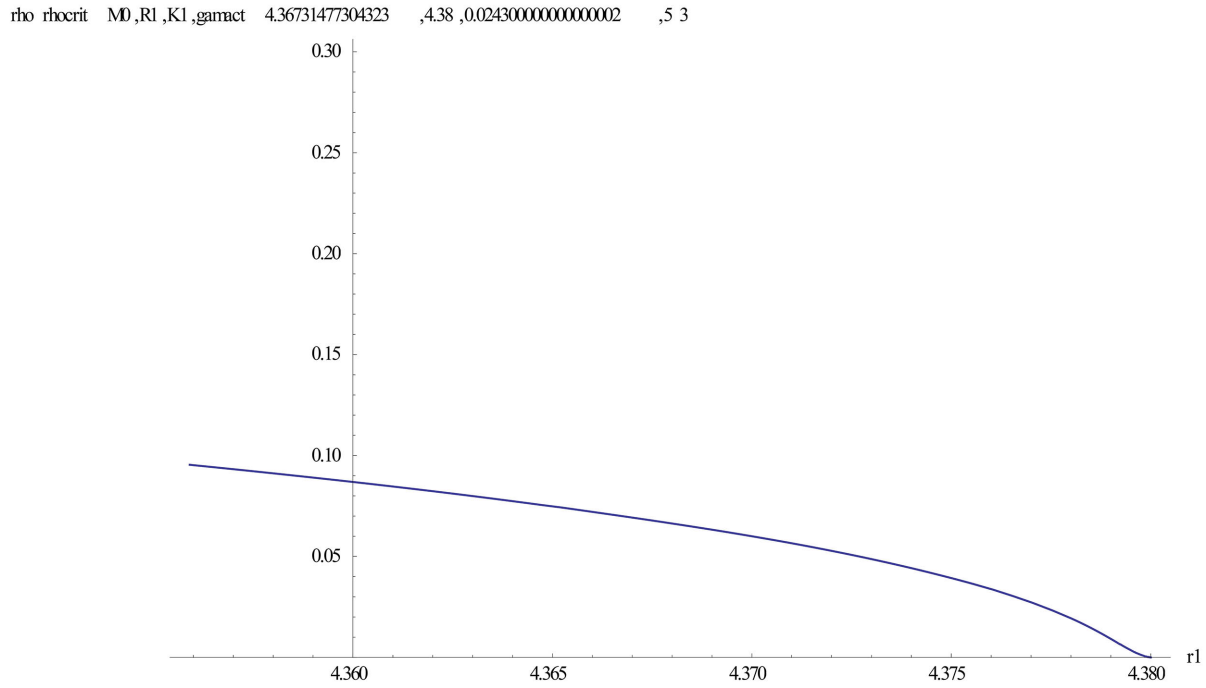

Figure 27. Typical galactic shell star: density in dependence of radius.

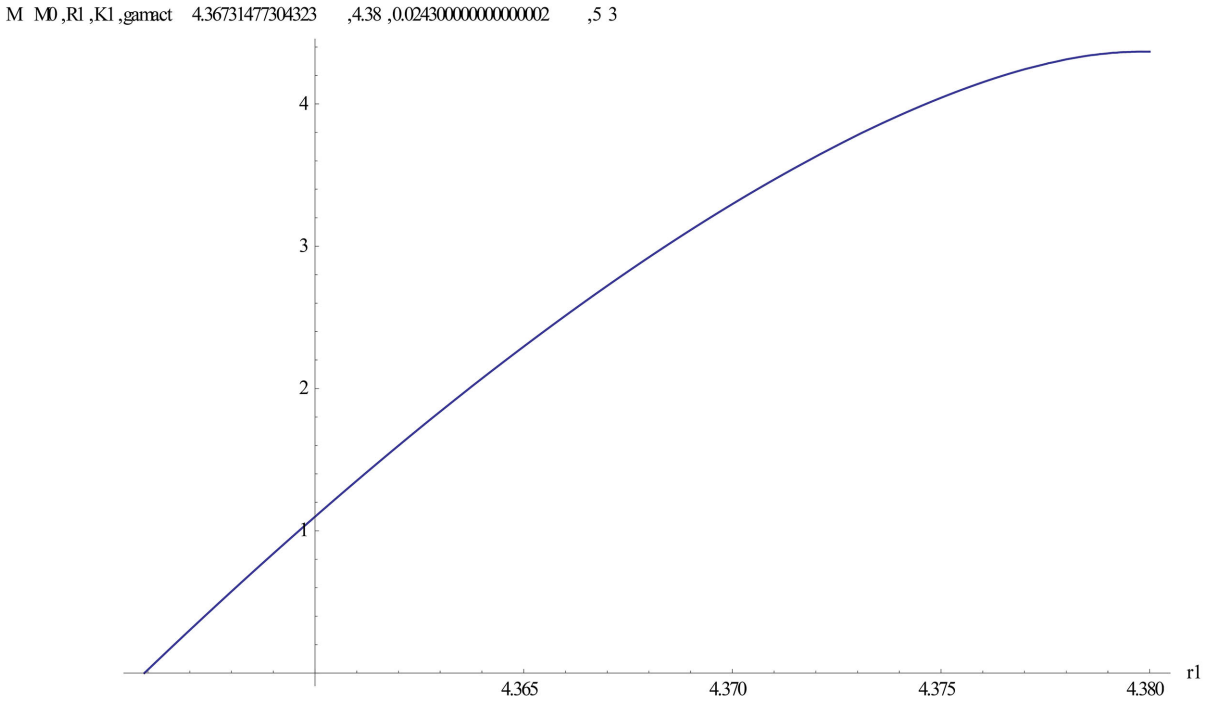

Figure 28. Typical galactic shell star: mass in dependence of radius.

$dR_{rel} = \left(R_1 - r_i\right)/M_0 = 0.00551$, the relative Schwarzschild-distance $dR_{srel} = \left(R_1 - M_0\right)/M_0 = 0.00290$, the light attenuation factor is roughly $1/dR_{srel}$ = 344.

Furthermore, r_i is little sensitive to the temperature up to $T = 10^7$ K.

As for a stellar black hole, when R converges to $r_s = M_0$, so does the inner radius r_i, and there is no physical solution (with positive ρ and M) for a boundary within the horizon.

8. The Three Star Models for Kerr-Space-Time with Mass and Rotation

The calculation of Kerr-space-time with mass and rotation was carried out for 3 star models:

- a typical compact neutron star with mass around 1 solar mass;
- a presumably typical stellar shell-star with a mass around 15 solar masses;
- a comparatively small galactic shell-star modelled on the central black-hole in the Milky Way with a mass of around 4 million solar masses.

The angular velocity ω was chosen at $0.36\omega_{max}$, *i.e.* about 1/3 of the maximum value.

We are using the so called "sun units" sun Schwarzschild-radius $r_{ss} = r_s\left(sun\right) = 3\,\text{km}$, sun mass $M_s = M\left(sun\right) = 3\times10^{30}\,\text{kg}$, sun Schwarzschild-density $\rho_s = \dfrac{M_s}{4\pi r_{ss}^3} = 1.76\times10^{16}\,\text{g/cm}^3$, sun Schwarzschild-pressure $P_s = \rho_s c^2 = 1.58\times10^{35}\,\text{J/m}^3$ for radius r, mass M, density ρ, and pressure P, respectively.

The mass element here is $M_1(r, \theta)\mathrm{d}r\mathrm{d}\theta$ and the ring mass $M_1(\theta)$ is the differential mass of the θ-beam $\mathrm{d}\theta M_1\left(\theta\right) = \mathrm{d}\theta M_1\left(R_1\left(\theta\right), \theta\right)$, the density ρ is $4\pi\,\text{Cos}\left(\theta\right)\rho\left(r,\theta\right)\mathrm{d}r\mathrm{d}\theta = \partial_r\partial_\theta M_1\left(r,\theta\right)$.

As for the result values, dthrel is the maximum relative angular deviation (in θ), and error (relative to the test function error): wavefront error is the median (on lattice) algorithm error, the interpolation and the Fourier fit error is the error of the respective fit of the discrete solution on the lattice.

We are using here the *θ-slicing r-backward algorithm* for the shell-stars. For each of the star models a *verification step* is run first with the angular velocity ω = 0, the result must be the same as in the corresponding TOV-equation. Then a parameter *case-study* is made for different outer boundary ellipticities ΔR_1 at the outer boundary condition in order to find ΔR_1*with a minimal mean energy density*: this is the stable solution of the Kerr-Einstein equations.

The algorithm yields as the result a pointwise array of values and first and second derivatives of the variables. The variables for the 6 Einstein equations are the 5 Kerr correction-factor functions $A0(r, \theta)$, …, $A4(r, \theta)$, and $\rho(r, \theta)$.

We are using the *θ-slicing r-forward algorithm* for the compact neutron star. The variables for the 6 Einstein equations are the 5 Kerr correction-factor functions $A0(r, \theta)$, …, $A4(r, \theta)$, and $M_1(r, \theta)$.

The value denomination is:

a = alpha1 with $a = \frac{J}{Mc}$ the angular momentum radius (amr) of the Kerr model,

ω = omega1 is the angular velocity, R_1 = R1 = r02 is the outer radius, M_0 = M0 is the total mass,

r_1 radius variable, th angle variable,

$M(r, \theta)$ = M1(r1, th) is the mass function, $A0(r, \theta)$, …, $A4(r, \theta)$ Kerr correction-factor functions,

$\rho(r, \theta)$ = rho(r1, th) is the density function,

k_1 is the parameter in the approximate Fermi-gas equation-of-state $P_1(r_1) = k_1 \rho_1(r_1)^{\gamma}$,

γ = gam, gam1, gam2 is the exponent,

infac is the moment of inertia factor α_i,

epsi is the singularity cancellation parameter with limit(epsi) = 0 introduced to improve the numerical stability in singularities

r_i = riact is the polar inner radius R_y

Δr_i the inner ellipticity is the difference between the polar r_{iy} and the equatorial inner radius r_{ix}, $\Delta r_i = r_{iy} - r_{ix}$

ΔR_1 Is the outer ellipticity, with outer radii $R_{x1} = R_1 - \Delta R_1$ and $R_{y1} = R_1$

rilow is the minimal radius r_1 reached in the solution

ρ_{bc} = rhobcx is the boundary condition density

dthrel is the maximum relative difference of a value dependent on θ, e.g.

dthrel(R_1) = (max($R_1(\theta)$) − min($R_1(\theta)$))/mean($R_1(\theta)$)

shell thickness $dR_1 = R_1(\theta) - \Delta r_i(\theta)$

Typical rotating compact neutron star

The underlying star model here is a compact (r_i = 0) neutron star of neutron liquid (*i.e.* strongly interacting neutrons), mass M_0 = 0.932 sun-masses, radius R_1 = 2.76 sun-Schwarzschild-radii r_{ss} (r_{ss} = 3.0 km), ω = 0.108688. The underlying calculation is the Mathematica-notebook [18], the results in [19].

The full parameters are:

{alpha1 = 0.331224, omega1 = 0.108688, k1 = 0.4, gam = 5/3., gam1 = 5/3., gam2 = 4/3., M0 = 0.932, dr02rel = 0.33, infac = 2/5., epsi = 0.1, rilow = 0.001, rhobcx = 0.0456}

The *r-forward* solution is first calculated with the lattice {n_x = 33, n_y = 17} for the rotation-free TOV-case with a TOV-solution as the initial function.

The solution for the Kerr-case starts with this corrected TOV-solution and yields the values:

outer radius $R_1(\theta) = \{2.83912, \cdots, 2.83722\}$, mean = 2.83897, dthrel = 0.00118.

total mass M02eff = 0.932.

error: med(err) = 0.0639 wavefront, = 0.0491 interpolation, = 0.0492 Fourier fit.

mean energy density = 0.0791.

The resulting density is depicted in **Figure 29**, mass M in **Figure 30**, and the

effective radius over azimuthal angle th in Figure 31.

The density distribution is similar to the TOV-case but with a decrease in θ-direction.

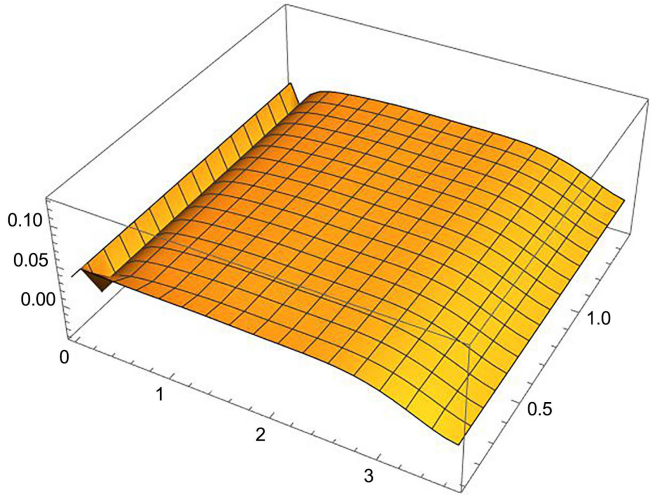

Figure 29. Typical rotating compact neutron star: density over x = radius r_1, y = angle th.

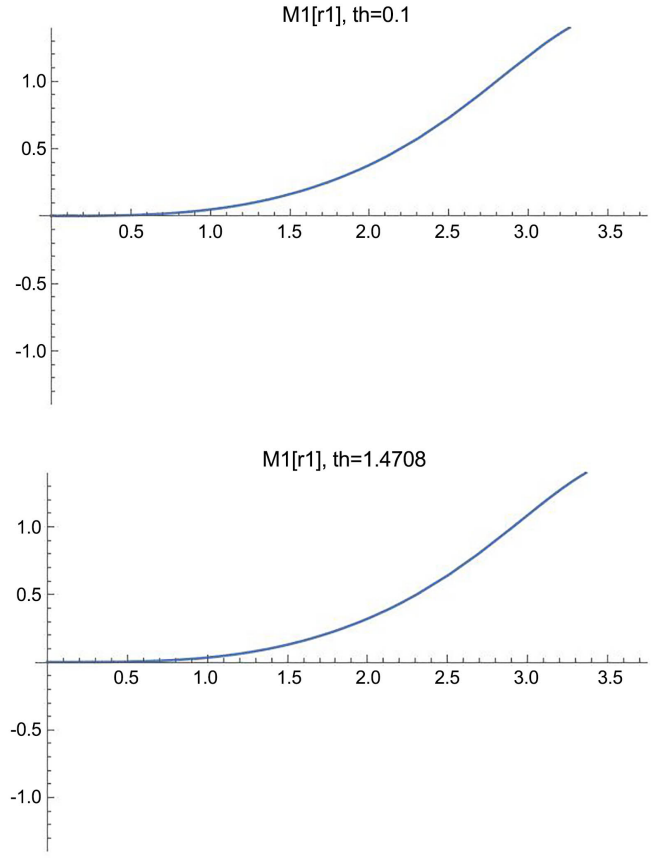

Figure 30. Typical rotating compact neutron star: (ring) mass profile for th = 0.1 (equatorial) and th = 1.4708 (polar), the outer edge is reached when $M_1(r_1) = M_0$.

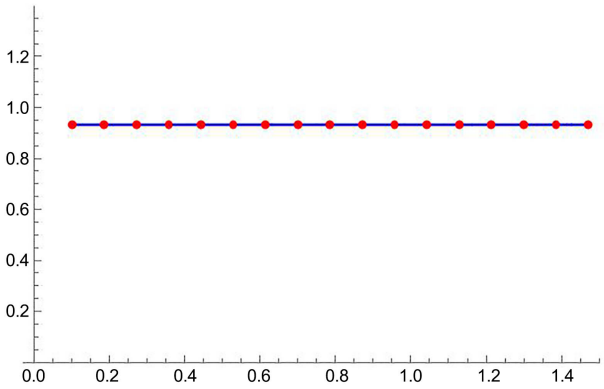

Figure 31. Typical rotating compact neutron star: effective radius r_{02e} over angle th.

The rotation results show very small flattening in the polar direction ofdthrel = 0.00118. The neutron star behaves like *a fluid* because of its "viscosity", that is, its nuclear interaction and becomes "pumpkin-like".

Typical rotating stellar shell-star

The star model here is a shell-star (r_i > Schwarzschild-radius) with mass M_0 = 15.69 sun-masses, radius R_1 = 17.89 sun-Schwarzschild-radii r_{ss}(r_{ss} = 3.0 km), and angular frequency ω = 0.0126.

The outer Kerr-horizon is r_+ = 15.21. The underlying calculation is the Mathematica-notebook [20], the results in [19].

The outer ellipticity ΔR_1 is at first a free parameter and calculated from a case-study of minimal mean energy density to $\Delta R_1 = 0.3 = 0.0168 R_1$.

The full parameters are

{apha1 = 2.68844, omega1 = 0.0126, k1 = 0.4, R1 = 17.89, gam = 5-/3., gam1 = 5/-3., gam2 = 4-/3., M0 = 15.69, infac = 2/-3., epsi = 0.1, rilow = 15.9, rhobcx = 0.036}

The *r-backward* solution is first calculated with the lattice {n_x = 17, n_y = 9} for the rotation-free TOV-case as the initial function.

Then a *case study* with the parameter ellipticity ΔR_1 is carried out in order to find the minimal mean energy density, on the set of values ΔR_1 = {0, −0.3, 0.3, 1., 1.6}

The case study yields a minimum at ΔR_1 = 0.3 (cigar-like outer boundary), with amean energy density = 0.017004.

This *energy-minimalsolution*with ΔR_1 = 0.3 yields the values:

outer radius $R_1(\theta) = \{17.59, \cdots, 17.89\}$, mean = 17.739, dthrel = 0.0164.

inner radius $r_i(\theta) = \{16.704, \cdots, 16.982\}$, mean = 16.823, dthrel = 0.0162.

total mass M02eff = 15.69, inner boundary max(ρ_{bc}) = 0.035955.

shell thickness dR_1: mean = 0.916, dthrel = 0.0448.

mean energy density = 0.0170.

error: med(err) = 0.00238 wavefront, = 0.00573 interpolation, = 0.00786 Fourier fit.

It is interesting to make a comparison with the *spherical-outer-boundary* so-

lution.

with $\Delta R_1 = 0$:

inner radius $r_i(\theta) = \{17.0033, \cdots, 17.0243\}$, mean = 17.020, dthrel = 0.00123.

total mass M02eff = 15.69, inner boundary max(ρ_{bc}) = 0.0375.

shell thickness dR_1: mean = 0.870, dthrel = 0.0241.

mean energy density = 0.017698.

error: med(err) = 0.00224 wavefront, = 0.00545 interpolation, = 0.0098 Fourier fit.

The solution with the next higher ellipticity $\Delta R_1 = 1.0$ has the values:

outer radius $R_1(\theta) = \{16.89, \cdots, 17.88\}$, mean = 17.38, dthrel = 0.055.

inner radius $r_i(\theta) = \{16.01, \cdots, 16.955\}$, mean = 16.438, dthrel = 0.0556.

total mass M02eff = 15.69, inner boundary max(ρ_{bc}) = 0.0359.

shell thickness dR_1: mean = 0.940, dthrel = 0.0894.

mean energy density = 0.017249.

error: med(err) = 0.00309 wavefront, = 0.00516 interpolation, = 0.00792 Fourier fit.

The two significant non-spherical features are the relative shell thickness variation dthrel(dR_1) and the relative inner ellipticity dthrel(r_i). The first depends roughly linearly on the outer ellipticity ΔR_1, plus the value at $\Delta R_1 = 0$ (dthrel(dR_1) = 0.0241), which is results from rotation. The second, dthrel(r_i), is almost equal to the relative outer ellipticity dthrel(r_i), plus the small amount at $\Delta R_1 = 0$ (dthrel(R_1) = 0.00123).

The density distribution is shown in **Figures 32-34**.

The density distribution increases in θ-direction ($\theta = 0$ is equatorial, $\theta = \pi/2$ axial).

The mass distribution is shown in **Figure 35**, **Figure 36**.

The physical mass distribution ends at the inner boundary at $r_i = 16.7$, where the density jumps to $\rho = 0$.

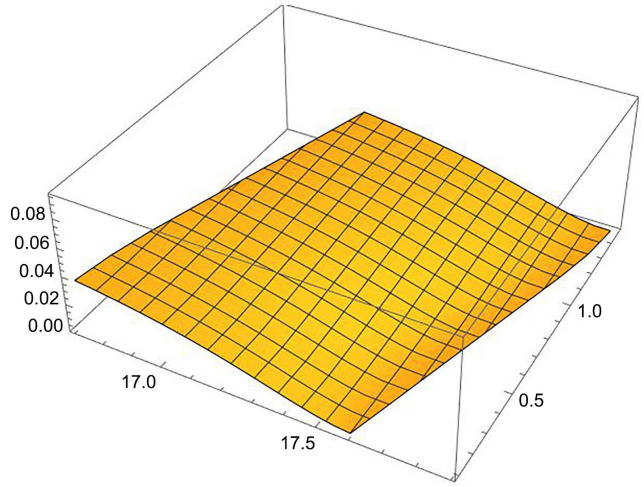

Figure 32. Typical rotating stellar shell star: density over x = radius r_1, y = angle th.

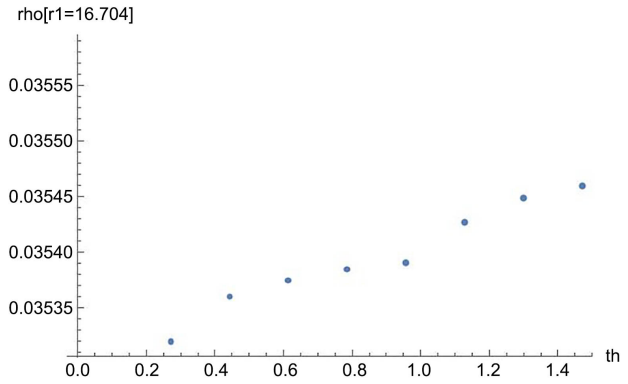

Figure 33. Typical rotating stellar shell star: density over angle th at the inner boundary $r_1 = 16.704$.

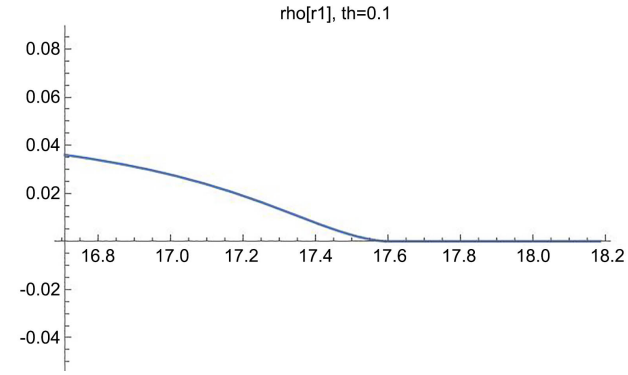

Figure 34. Typical rotating stellar shell star: the fitted density profile for th = 0.1 (equatorial).

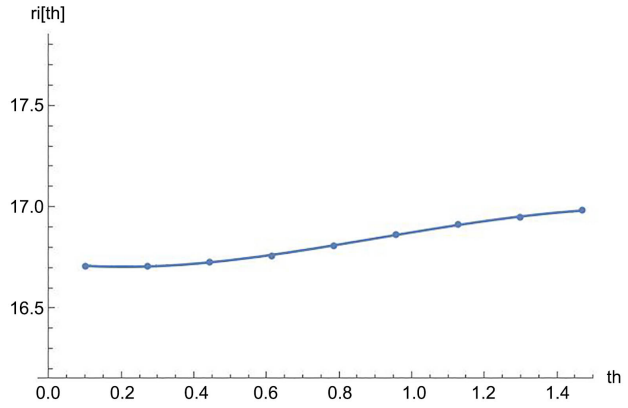

Figure 35. Typical rotating stellar shell star: effective inner radius r_i over angle th.

A remarkable result, distinct from the case of the neutron star, is the shape with rotation. The energy-minimal stellar shell-star behaves like a *ball of neutron gas* (negligible interaction) and decreases slightly its equatorial radius, so that, speaking naively, the increased gravitation counteracts the centrifugal force, the shell-star becomes "cigar-like", with the shell thickness approximately constant.

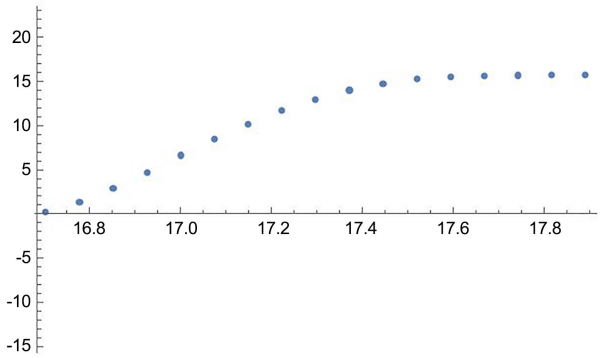

Figure 36. Typical rotating stellar shell star: Fourier-fitted total mass in dependence of radius.

The stellar shell-star has all its mass concentrated within a thin shell ($dR_1 = 0.916$) which is situated outside its Schwarzschild-radius $M_0 = 15.69$, where the minimum distance from the horizon is

$\min(R_1(\theta)) - M_0 = 1.01$,

therefore the light energy loss is approximately (in Newtonian approximation) $M_0/\min(R_1(\theta)) = 0.9395$ and the attenuation factor $1/(1 - M_0/\min(R_1(\theta))) = 16.53$, it means that visible green light of 0.514 μm is shifted to 8.50 μm into middle-range infrared.

Typical rotating galactic shell-star

This is modelled (approximately) on the central black-hole in the Milky Way with mass $M_0 = 4.36$ mega-sun-masses (MM_s), radius $R_1 = 4.38$ mega-sun-Schwarzschild-radii (13.14×10^6 km, Mr_{ss}) [21].

The underlying calculation is the Mathematica-notebook [22], the results in [23].

The outer Kerr-horizon is $r_+ = 4.26 Mr_{ss}$.

In order to maintain numerical performance, we are using for mass and distance 10^6 (mega) units 10^6 M_s and 10^6 r_{ss} and for density 10^{-12} (mega^{-2}) unit 10^{-12} ρ_s.

Like in the case of the stellar shell-star, the outer ellipticity ΔR_1 is at first a free parameter and calculated from a case-study of minimal mean energy density to $\Delta R_1 = -2$ dTOV, where dTOV is the shell thickness of the spherical shell-star dTOV = 0.057.

The full parameters are:

{alpha1 = 0.670047, omega1 = 0.05239, k1 = 0.0243, k2 = 0.067, $R1 = 4.38$, gam =, 5-/3,

gam1 =, 5/-3, gam2 =, 4-/3, M0 = 4.36731, infac =, 2/-3., epsi = 0.0024, rilow = 4.3, rhobcx = 4.915}

The *r-backward* solution is first calculated with the lattice $\{n_x = 17, n_y = 9\}$ for the rotation-free TOV-case as the initial function.

Then a *case study* with the parameter ellipticity ΔR_1 is carried out in order to find the minimal mean energy density, on the set of values $\Delta R_1 = \{0.1, -0.3, -1, -2\}$*dTOV.

The case study yields a minimum at $\Delta R_1 = -2$ dTOV $= -0.114$ (pancake-like

outer boundary), with a mean energy density = 1.734.

This *energy-minimalsolution* yields the values:

outer radius $R_1(\theta) = \{4.494, \cdots, 4.38\}$, mean = 4.43654, dthrel = 0.025367.

inner radius $r_i(\theta) = \{4.46456, \cdots, 4.34109\}$, mean = 4.40029, dthrel = 0.02765.

total mass M02eff = 4.3673, inner boundary max(ρ_{bc}) = 4.96075.

shell thickness dR_1: mean = 0.035256, dthrel = 0.2507.

mean energy density = 1.73479.

error: med(err) = 0.0122 wavefront, = 0.000404 interpolation, = 0.000437 Fourier fit.

In comparison, the *spherical-outer-boundary* solution with $\Delta R_1 = 0$ yields the values:

inner radius $r_i(\theta)$ = {4.34861, …, 4.3423}, mean = 4.343, dthrel = 0.00145.

total mass M02eff = 4.36731, inner boundary max(ρ_{bc}) = 4.68324.

shell thickness dR_1: mean = 0.0370, dthrel = 0.1736.

mean energy density = 1.75914.

error: med(err) = 0.0101 wavefront, = 0.000390 interpolation, = 0.000324 Fourier fit.

In contrast to the stellar shell-star, here the relative variation of the shell thickness for the spherical-outer-boundarysolution is smaller by a factor of 20 as compared to the minimal solution with a high outer ellipticity, so here there is a dependence of the shell thickness on the ellipticity.

The density distribution is shown in **Figures 37-39**.

The density distribution increases in th-direction.

The mass distribution is shown in **Figure 40**, **Figure 41**.

The physical mass distribution ends at the inner boundary at r_i = 4.46456, where the density jumps to $\rho = 0$. The fit extrapolates it to lower r-values.

The maximum distance from the horizon is max(r_{02e}) − r_+ = 0.125, therefore the minimal light energy attenuation is roughly 4.262/0.125 = 34, it means that visible green light of 0.514 μm is shifted to 17 μm into far-infrared.

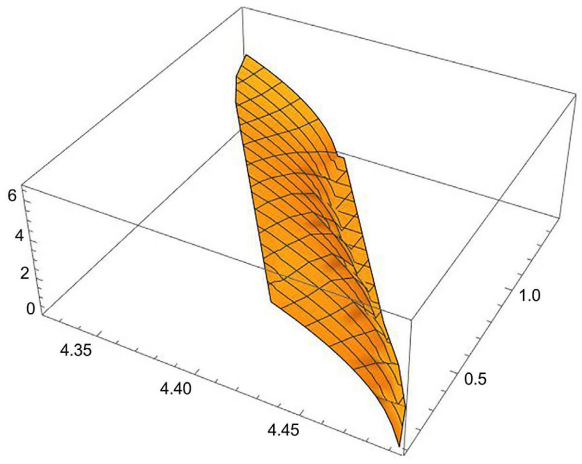

Figure 37. Typical rotating galactic shell star: density over x = radius r_1, y = angle th, radius in mega-r_s(sun)=3 10^6 km, th in radian.

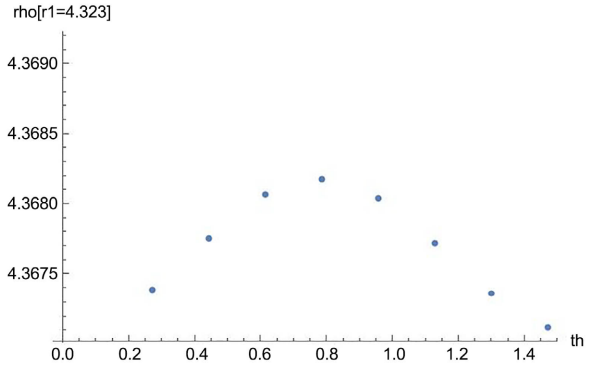

Figure 38. Typical rotating galactic shell star: density over angle th at the inner boundary r_1 = 4.464, radius in mega-r_s(sun)=3 10^6 km, th in radian.

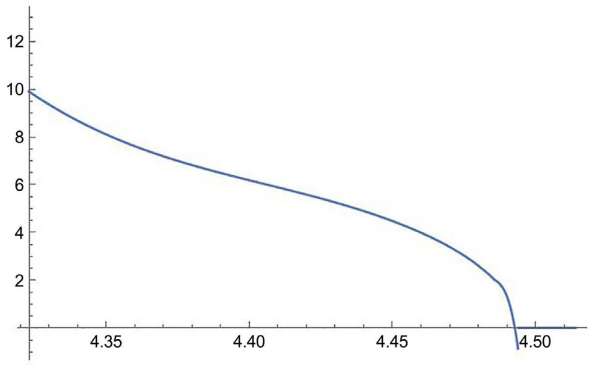

Figure 39. Typical rotating galactic shell star: fitted density profile for th = 0.1 (equatorial), radius in mega-r_s(sun)=3 10^6 km, th in radian.

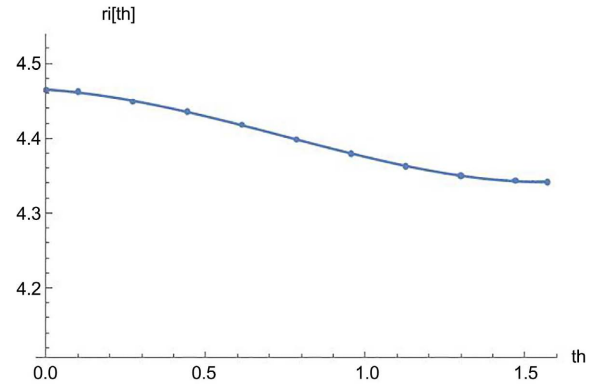

Figure 40. Typical rotating galactic shell star: inner radius r_i over angle th, radius in mega-r_s(sun)=3 10^6 km, th in radian.

The galactic shell-star has all its mass concentrated within a thin shell (dR_1 = 0.0362) which has its inner radius inside and its outer radius outside its Schwarzschild-radius M_0 = 4.367, where the minimum distance from the horizon is

$\min(R_1(\theta)) - M_0 = 0.0127$,

therefore the light energy loss is approximately (in Newtonian approximation)

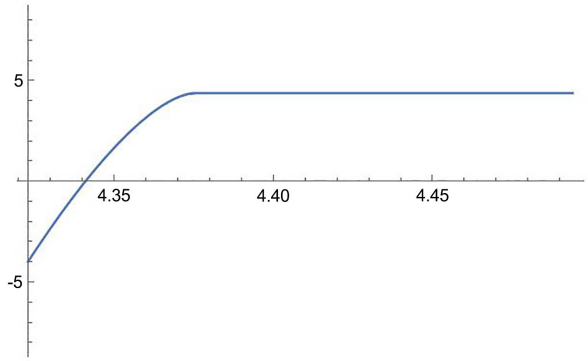

Figure 41. Typical rotating galactic shell star: total mass $M_1(r_1)$ over radius, radius in r_s(sun)=3 km, th in radian.

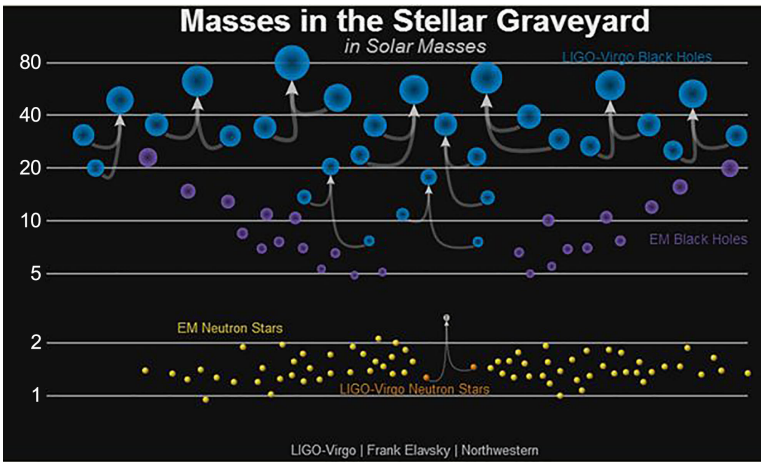

Figure 42. Mass distribution of stellar black-holes and neutron stars measured by LIGO.

$M_0/\min(R_1(\theta))$ = 0.9971 and the attenuation factor $1/(1 - M_0/\min(R_1(\theta)))$ = 345, it means that x-ray-radiation from in-falling matter from the accretion disc with an energy of 5 keV and λ = 0.2 nm is shifted to λ = 69 nm, that is into hard UV-radiation.

9. Experimental Evidence with Recent LIGO and X-Ray Measurements

In November 2018, the LIGO cooperation published the newest statistics of neutron stars and black holes, based on gravitational waves and x-ray measurements [24].

The resulting mass distribution for black-holes and neutron stars is shown in **Figure 42** [24].

From these results, we can deduce a confirmed mass range for neutron stars of $0.9M_{sun} \le M_{ns} \le 2.9M_{sun}$ and for stellar black holes $5M_{sun} \le M_{bh} \le 80M_{sun}$.

This mass range confirms our results from chapter 7 *for compact neutron stars in the range* $M \le 3.04M_{sun}$, but not for the neutron shell stars in the range $3.04M_{sun} \le M \le 4.91M_{sun}$.

It means that the fluid (non-compact) shell stars are not stable, and only Fermi-gas shell stars are stable.

The mass range *for stellar shell star black holes* deduced in chapter 7:

$5.5M_{sun} \le M_{bh} \le 81.3M_{sun}$ *is confirmed*, considering that the uncertainty of mass measurement via x-rays is easily $\delta M_{bh} \ge 0.5M_{sun}$.

10. Conclusions

We introduce in chap. 6 an eos for the nucleon-fluid in the density range $\rho_c \le \rho \le \rho_m$, where $\rho_c = 0.0417\rho_s$ and $\rho_m = 0.0544\rho_s$ (sun units $r_{ss} = 3$ km, $\rho_s = 1.76 \times 10^{16}$ g/cm^3), which is based on measurement data for the nucleon-nucleon-potential. This suggests, that there is a phase transition at $\rho = \rho_c$ from the (interacting) nucleon fluid to the (weakly interacting) nucleon Fermi-gas.

Based on these 2 eos's the results for the TOV-equation in chap. 7 are as follows.

Neutron stars obey the nucleon fluid eos and there are compact neutron stars in the range $(M_0, R_1) = (0.14M_{sun}, 1.49r_{ss}), \ldots, (3.04M_{sun}, 3.95r_{ss})$, the *R-M*-relation follows approximately a cubic-root-law: $R \sim M^{1/3}$.

Neutron shell-stars in the range $(M_0, R_1) = (3.04M_{sun}, 3.95r_{ss}), \ldots, (4.91M_{sun}, 4.92r_{ss})$ are not stable.

Stellar shell-stars exist in the range of $(M_0, R_1) = (5.5M_{sun}, 9.1r_{ss}), \ldots, (81.3M_{sun}, 91.2r_{ss})$.

The underlying equation-of-state is the Fermi-gas of nucleons with the eos $P(\rho) = K_1\rho^{5/3}$. The resulting R-M-relation is practically linear and has a maximum mass value of $M_{max} = 81.3M_{sun}$. The light attenuation factor (redshift) is roughly {1.7, …, 50}. Taken the redshift and the small relative shell thickness of around 0.02, these stellar shell-stars have approximately the properties expected of a genuine black-hole, when measured from a distance $r \gg R_1$. Furthermore, the phase space volume of a thin spherical shell is proportional to its surface A, which approximates the Bekenstein-Hawking black-hole entropy formula $S = \left(k_B / L_P^2\right) A/4$.

The galactic (supermassive) shell-stars have the density scale and the eos of a white-dwarf-star, *i.e.* of an electron Fermi-gas. The *R-M*-relation is almost linear and goes from $1MM_{sun}$ up to $50MM_{sun}$ ($MM_{sun} = 10^6 M_{sun}$, $Mr_{ss} = 10^6 r_{ss}$). $dR_{rel} = (R_1 - r_i)/M_0$ is the relative thickness, and shows, that the shells are very thin indeed, with a minimum of 0.001. The relative Schwarzschild-distance $dR_{srel} = (R_1 - M_0)/M_0$ has a minimum at $\{M_0, dR_{srel}\} = \{7MM_{sun}, 0.00142857\}$, the redshift is around 700. So the overall result is, that the supermassive shell-stars become ever thinner shells, while the distance from the Schwarzschild-horizon is increasing.

In chap. 8 we present numerical results for rotating stars of the 3 types compact neutron star, stellar shell-star and galactic shell-star.

The angular velocity ω was chosen at $\omega = 0.36\omega_{max}$, *i.e.* about 1/3 of the maximum.

The compact neutron star with $M_0 = 0.932 M_{sun}$, $R_{1y} = 2.8372 r_{ss} = 8.51$ km, $R_{1x} = 2.8391 r_{ss}$, $\omega = 0.1087$, has the relative ellipticity of dthrel = 0.00118. The neutron star behaves like *a fluid* because of its "viscosity", that is, its nuclear interaction, and becomes slightly "pumpkin-like".

The stellar shell-star with $M_0 = 15.74 M_{sun}$, $R_{1mean} = 17.74 r_{ss}$, $\omega = 0.0126$, has maximum density $\rho_{bc} = 0.03595 \rho_s$, outer radii $R_{1y} = 17.89 r_{ss} = 53.67$ km, $R_{1x} = 17.59 r_{ss}$, inner radii $r_{iy} = 16.98 r_{ss}$, $r_{ix} = 16.70 r_{ss}$, inner rel. ellipticity dthrel = 0.0162. The redshift is 16.53.

The stellar shell-star behaves like a *ball of neutron gas* (negligible interaction) and decreases slightly its equatorial radius, so that, speaking naively, the increased gravitation counteracts the centrifugal force, the shell-star becomes "cigar-like", with the shell thickness approximately constant.

The galactic shell-staris modelled (approximately) on the central black-hole in the Milky Way with mass $M_0 = 4.368 MM_{sun}$ ($MM_{sun} = 10^6 M_{sun}$, $Mr_{ss} = 10^6 r_{ss}$), radius $R_1 = 4.38 Mr_{ss}$ (=13.14 × 10^6 km), $\omega = 0.05239$.

It has maximum density $\rho_{bc} = 4.961 \times 10^{-12} \rho_s$, outer radii $R_{1y} = 4.38 Mr_{ss}$, $R_{1x} = 4.494 Mr_{ss}$, inner radii $r_{iy} = 4.341 Mr_{ss}$, $r_{ix} = 4.464 Mr_{ss}$, inner rel. ellipticity dthrel = 0.0276.

The redshift is roughly 345. The galactic shell-star is a shell object with a thin mass shell ($\Delta R = 0.0352 Mr_{ss}$) situated close above its outer Kerr horizon $r_+ = 4.26 Mr_{ss}$. The polar radius is smaller than the equatorial radius, so the outer shape and the inner shape are both *pancake-like*.

The overall result is, that the introduction of numerical shell-star solutions of the TOV- and Kerr-Einstein-equations creates shell-star star models, which mimic closely the behaviour of abstract black holes and satisfy the Bekenstein_Hawking entropy formula, but have finite redshifts and escape velocity $v < c$, no singularity, no information loss paradox, and are classical objects, which need no recourse to quantum gravity to explain their behaviour.

Conflicts of Interest

The author declares no conflicts of interest regarding the publication of this paper.

References

[1] Fliessbach, T. (1990) Allgemeine Relativitätstheorie. Bibliographisches Institut, Leipzig.

[2] Lattimer, J.M. and Prakash, M. (2000) Neutron Star Structure.

[3] Visser, M. (2008) The Kerr Spacetime: A Brief Introduction.

[4] Kokkotas, K.D. and Vavoulidis, M. (2005) Rotating Relativistic Stars. *Journal of Physics*, *Conference Series*, **8**, 71-80. https://doi.org/10.1088/1742-6596/8/1/009

[5] Wasserman, A.L. (2011) Thermal Physics. Oregon State University, Corvallis. https://doi.org/10.1017/CBO9780511902611

[6] Helm, J. (2022) Mathematica-Notebook GRSchwarzTOVOrig3.nb. https://www.researchgate.net/publication/358270854_Star_models_as_solutions_of

_TOV-equation, calculation for non-rotating star-models

[7] Papenbrock, Th. (2008) Physics of Nuclei. National Nuclear Physics Summer School.

[8] Steiner, A.W., Hempel, M. and Fischer, T. (2013) Core-Collapse Supernova Equations of State Based on Neutron Star Observations. *The Astrophysical Journal*, **774**, Article No. 17. https://doi.org/10.1088/0004-637X/774/1/17

[9] Hempel, M. (2014) Materie am Limit. *Physik in unserer Zeit*, **45**, 12-20. https://doi.org/10.1002/piuz.201301352

[10] Hjorth-Jensen, M. (2007) Models for Nuclear Interactions. arxiv-nucl-th9811101.

[11] Douchin, F. and Haensel, P. (2001) A Unified Equation of State of Dense Matter and Neutron Star Structure. *Astronomy and Astrophysics*, **380**, 151-167.

[12] Rosenfield, P. (2007) Properties of Rotating Neutron Stars. PhD Thesis, University of Washington, Seattle.

[13] Urbanec, M. (2010) Equations of State and Structure of Neutron Stars. PhD Thesis, Silesian University in Opava, Opava.

[14] Stergioulas, N. (2003) Rotating Stars in Relativity. *Living Reviews in Relativity*, **6**, Article No. 3. https://doi.org/10.12942/lrr-2003-3

[15] Dain, S. (2012) Geometric Inequalities for Axially Symmetric Black Holes. *Classical and Quantum Gravity*, **29**, Article ID: 073001.

[16] Typel, S., *et al.* (2010) Composition and Thermodynamics of Nuclear Matter with Light Clusters. *Physical Review C*, **81**, Article ID: 015803. https://doi.org/10.1103/PhysRevC.81.015803

[17] Chandrasekhar, S. (1992) The Mathematical Theory of Black Holes. Oxford University Press, Oxford.

[18] Helm, J. (2022) Mathematica-Notebook KerrBLS2e.nb. https://www.researchgate.net/publication/358270862_Star_models_as_solutions_of_Kerr-spacetime_with_matter, calculation for rotating compact neutron-star

[19] Helm, J. (2022) word-doc KerrBLS_Results.doc. https://www.researchgate.net/publication/358270862_Star_models_as_solutions_of_Kerr-spacetime_with_matter, concise results for rotating star-models

[20] Helm, J. (2022) Mathematica-Notebook KerrBLS0e.nb. https://www.researchgate.net/publication/358270862_Star_models_as_solutions_of_Kerr-spacetime_with_matter, calculation for rotating shell-star

[21] Ferrarese, L. and Merritt, D. (2002) Supermassive Black Holes. *Physics World*, **15**, 41-46.

[22] Helm, J. (2022) Mathematica-Notebook KerrBLS1e.nb. https://www.researchgate.net/publication/358270862_Star_models_as_solutions_of_Kerr-spacetime_with_matter, calculation for rotating galactic shell-star

[23] Helm, J. (2022) Mathematica-Notebook KerrBLS1e.nb.

[24] LIGO Cooperation (2018, November). https://www.ligo.caltech.edu/image/ligo20171016a